4-22-2021

Surface Functionalization of Elastomers for Tunable Crystal Growth and Smart Adhesives

John Kapitan
University of Nebraska-Lincoln, jkapitan@huskers.unl.edu

SURFACE FUNCTIONALIZATION OF ELASTOMERS FOR TUNABLE CRYSTAL GROWTH AND SMART ADHESIVES

By

John M. Kapitan

A THESIS

Presented to the Faculty of

The Graduate College of the University of Nebraska

In Partial Fulfillment of Requirements

For the Degree of Master of Science

Major: Chemistry

Under the Supervision of Stephen A. Morin

Lincoln, Nebraska

April, 2021

SURFACE FUNCTIONALIZATION OF ELASTOMERS FOR TUNABLE CRYSTAL GROWTH AND SMART ADHESIVES

John M. Kapitan, M.S.

University of Nebraska, 2021

Advisor: Stephen A. Morin

Silicone rubbers have seen extensive work on modulation of their surface environments for use in microfluidics, cell adhesion, and sensing. Most surface procedures utilize a common initial step of oxidation of the surface to increase the number of active surface functional groups. Following oxidation more permanent functionalities can be imparted on the surface using silanization, grafting polymer brushes, or creating ionic bonds to the surface. Of these three, silanization proves to be the most pervasive due to the range of procedures available and how easy the procedures prove to be. However, the mechanism by which silanization is performed heavily involves reactivity with alcohol groups making the procedure unavailable to functional groups containing alcohols and functional groups that share similar structural features. Expanding the scope of functional groups available through silanization can be achieved by attaching groups to the surface that can be easily replaced or transformed. Increasing the scope of available surface functional groups was achieved by using the copper catalyzed azide-alkyne click reaction.

Controlling the areas that reactivity occurs at, by using patterning techniques, allow for the generation of distinct regimes of surface chemistry. This can allow for

wholly new surface functions such as the ordering of large arrays of liquid droplets, directional control of the movement of droplets across the surface, and control over the adhesive forces the surface experiences. Combining chemical patterning with physical patterning, selective removal of contact areas, allowed for fine tuning of the adhesive properties and produced a favorable delamination axis. The work outlined here is applicable to a broad range of fields including, biomineralization, biomaterial engineering, and adhesive design.

ACKNOWLEDGEMENTS

The work involved in preparing, writing, and defending this thesis was not mine alone and I would like to take a moment to recognize and thank some of the people who helped me accomplish this task.

First, I want to thank my parents, Deborah and James Kapitan, for fostering my love and curiosity of science. From accidentally letting me watch Jurassic Park as a kid to agreeing to serve as a sounding board when I needed to verbalize the work featured in this document, without your constant love and support I would not be close to the individual I am today. Additionally, I would like to thank my siblings and grandparents for helping me to take the time to appreciate and take pride in myself and my accomplishments.

Next, I would like to thank Professor Stephen Morin for helping me transition into the scientist I am now. The breath of techniques and information I have learned under your tutelage is too numerous to mention here, but I want to make special mention of how you have taught to be more confident in myself and the work that I perform. Truly, thank you for all the help you have given me.

I also would like to take a moment to thank all of my friends and colleagues from my time working at the University of Nebraska, particularly my fellow members of the Morin group. First, I would like to thank Jay Taylor and Mark Rose who, despite having left the group, continue to be my friends, and serve as inspiration for who I strive to become. Without them I am not sure if I would have made it to this point as prepared as I am. Second, I would like to thank Abhiteja Konda, Joe Bowen, and Michael Stoller for

helping me feel welcomed in the group when I first joined and helping me to learn to work in a research laboratory. Lastly, I would like to thank the current members of the group, Ali Mazaltarim and Jessica Wagner, for their companionship and help with some of the projects featured.

I cannot express how truly fortunate I feel to have interacted with so many people who have impacted my life such positive ways. I only hope that I return this kindness and be a similarly positive force in the lives of others.

-John Kapitan (April 2021)

PREFACE

Study of the functionalization of surfaces is necessary to impart control over of how it might interact with other surfaces such as the nucleating crystals or adhering to other surfaces. While the functionalization of silicone elastomers is a well-defined field, the mechanism of binding organo-silanes to their surface provides a substantial obstacle to overcome. The attachment of functional groups not available by standard functionalization techniques proves the basis for much of my research.

Chapter 1 provides a comprehensive review of classical techniques for the functionalization of silicone elastomers. This includes covalent bonding strategies like oxidation, Self-Assembled Monolayers, grafting polymer brushes, ionic methods like successive ionic layer adsorption and reaction, layer by layer deposition, and strategies that cannot be considered covalent or ionic in their approach. These methods alone provide homogeneous surfaces that lack complexity in their response, so patterning techniques to create more complex surfaces, either by creating distinct regimes of surface chemistry or the generation of gradient surface chemistries, are also discussed. Applications of these techniques is also discussed to establish their current practical uses.

Chapter 2 is an overview of surface functionalization techniques for the expansion of available surface functional groups and adhesive force experienced by silicone elastomers. Increasing the scope of available functional groups is accomplished by using the copper-catalyzed azide alkyne click reaction. The success of this reaction was monitored using x-ray photoelectron spectroscopy to accurately measure the changes the surface of the elastomer experiences. Besides silicone elastomers, the commercial plastic poly (ethylene terephthalate) was derivatized using classical functionalization methods.

In Chapter 3, applications of these techniques is explored through biomineralization and adhesive force studies. Biomineralization rates can be controlled by performing the click reaction in the presence of different functional groups. Specifically, binding a carboxylic acid provides higher growth rates than native surfaces while binding alcohols creates an environment where little to no growth occurs. Introducing strain to samples prepared using the click reaction could provide a dynamic surface for biomineralization and allow for in situ control of nucleation rates. Adhesion is shown to be tunable by demonstrating a difference in peak delamination depending on the orientation and shape of the patten. Further tuning of functionalization techniques or use of more complex patterns could allow for a more dramatic peak force difference depending on the direction of delamination.

Finally, Chapter 4 posits how functionalization and patterning techniques of elastomeric substrates can be developed in the future. We look at preliminary findings supporting surface functionalization for the covalent binding of hydrogel microdroplets to the surface of elastomers. These droplets can be crosslinked and continue to swell and deswell in a manner like those prepared in bulk. Separately, a hydrogel system utilizing similar binding chemistries can also be deposited and crosslinked to the surface of silicone elastomers. This hydrogel, poly (ethylene glycol) diacrylate, also features high biocompatibility and will be used for the creation of a three-dimensional growth scaffold for cells trapped in the polymer matrix.

Additional Comments

- Chapter 1 is an invited review in preparation by me for *Journal of Materials Chemistry C*, in collaboration with A. Mazaltarim, J. Wagner, and S. A. Morin

- Chapter 2 is divided into two projects: the first is a manuscript in preparation outlining the use of the click reaction in collaboration with J. Tayler and S. A. Morin, the second is a collaborative project with the Bartlet group from Iowa State University
- Chapter 3 is divided into the same components as chapter 2 while focusing on applications of the techniques outlined in the preceding chapter.
- Chapter 4 begins with a publication in preparation in collaboration with M. Rose and S. A. Morin
- Chapter 4 also contains a collaborative project with R. Yang in engineering.

TABLE OF CONTENTS

LIST OF FIGURES

CHAPTER 1: SURFACE CHEMICAL MODIFICATIONS OF SILICONE ELASTOMERS TOWARDS CHEMICALLY ADAPTABLE MATERIALS

Materials used in applications such as biomedical implants[1-2], next-generation smart adhesives[3-4], and soft robotics[5-6], require specific surface and bulk properties. Elastomeric polymers (elastomers) are materials that have been used for these applications due to their high yield points[7-8], adaptable surfaces[9-10], and ease of manufacturing. Elastomers encompasses a very wide range of polymeric structures including poly(isoprenes)[11], poly(urethanes)[12], and silicone rubbers[13]. Silicone rubbers in particular feature a highly tunable chemical structure with a variety of monomers, catalysts, and vulcanization techniques[13-14]. This work is limited in scope to the room temperature vulcanization 2 component (RTV2) rubber Sylgard 184, often referred to as poly (dimethyl siloxane) or PDMS, due to its pervasiveness in the field and large body of previous work[13-16].

This chapter aims to present a comprehensive review of chemical modifications of the surface of silicone elastomers, particularly PDMS, including covalent, ionic, and methods that do not fit in the previous categories. Utilization of different patterning techniques, such as masking and gradients, will be discussed to demonstrate generation of heterogeneous surfaces. Applications of these functionalization and patterning techniques will be highlighted, particularly their use in biomaterials, heterogeneous catalysis, and soft robotics.

1.1 Surface Chemical Modification of Elastomeric Polymers

The most extensively studied method of surface chemical modifications is to create covalent bonds to the surface of the elastomer. Since the initial surface state of elastomers, such as PDMS, is often inert to chemical treatment an initial treatment can be required to create functional bonds to the surface[17]. Beginning with oxidation is the most common means of initial functionalization because it is an easy and straightforward procedure. The two most common methods of oxidation are the use of high energy plasma and ultra-violet oxidation.

High energy plasma can be performed with several different gases, such as oxygen[17], argon[18], or nitrogen[19], while the gas may vary most share the common trait of increasing the hydrophilicity of PDMS[20]. A large benefit of this method is that it can be performed incredibly quickly, often in less than 1 minute. When using oxygen plasma specifically, the surface experiences a transformation to form silanol, SiOH, groups on the surface which increases the surfaces' ability to partake in hydrogen bonding. A side effect of this treatment is the formation of a brittle silica layer on the surface[21]. Which in turn can lead to cracking[22] on the surface as silica has a much lower yield point than PDMS, this however can be alleviated by reactive ion etching[23] of the surface. Suspending plasma oxidized PDMS in an ionic solution, a common solution is phosphate buffer solution (PBS), will result in the gradual removal of the silica layer[24]. This process can be quickened using heat[24], however that may also lead to the surface returning to its native state entirely reversing the oxidation procedure.

An alternative to plasma oxidation, ultraviolet light can also be used to oxidize the surface of elastomers. The mechanism of ultraviolet oxidation (UVO) is not very well

understood but is believed to be triggered by the formation of ozone by the UV source to create reactive oxygen species that form silanol groups[25,26]. This results in a surface that is compositionally similar to one treated with oxygen plasma. Derivatization by this scheme is considerably more time consuming than plasma but does not result in formation of the brittle silica layer. Neither of these oxidation procedures result in permanent surface transformations[27]. Often, the surface will slowly rearrange and subsume the pendant silanol groups back into the bulk returning to its initial surface chemical state.

Following oxidation with another surface functionalization technique is often performed to create surfaces more permanently transformed than oxidation alone can manage. A common post-oxidation functionalization technique is the use of self-assembled monolayers (SAMs). SAMs were originally used by Whitesides[28] for the functionalization of gold. This functionalization utilized the affinity between gold and sulfur to bind long chain alkyl thiols[29,30], affecting the hydrophobicity of the surface. Due to the long alkyl chains on the surface these alkane-thiols resulted in much more permanent transformations to the surface, serving as long-lasting functional coatings.

SAMs eventually saw application on silicones with the use of organo-silanes[31-33]. Structurally organo-silanes are a fully bonded silicon with three of those bonds constituting either a halogen or an ether with the fourth group being the functional group of interest. Bonding of the organo-silane to the surface is typically performed one of two ways, either by liquid or vapor deposition[34]. Liquid deposition of silanes typically uses a mixture of ethanol and water to suspend the silane while the sample is submerged into the mixture for several minutes. Following the submersion, the sample is placed in an oven to

facilitate the dehydration reaction and create the silyl ether bonds. Vapor deposition of silanes involves use of a low-pressure vacuum to vaporize the silane and react with an oxidized surface in the gaseous state[35]. This does not require the use of an oven to facilitate the dehydration reaction but can be difficult as silanes typically have low surface tensions even at low pressure. Irrespective the deposition method, organo-silanes form stable silyl ethers with the surface of the oxidized silicone

Compared to just oxidation techniques, the main advantage that SAMs give is that they allow the user to create more permanent surfaces that, depending on the silane, can yield more exotic functionalities than oxidized or native surfaces alone[36]. (3-amino propyl) triethoxy silane (APTES) has been used in our group[37] to bind fluoresceine isothiocyanate (FITC) to the surface of PDMS. APTES can also be used to create long-lasting surfaces for the anchoring of cell adhesion promotion proteins[38]. The main issue that SAM's meet in current applications is through the bonding mechanism. Since the primary attachment mechanism relies heavily on the dehydration reaction of silyl alcohols[39] this makes it incredibly difficult to utilize silanes containing terminal alcohols and similar functional groups.

Using pre-synthesized molecules for the functionalization or PDMS is not exclusive to SAMs. Polymer brushes can also be used for surface functionalization[40]. Functionalization using polymer brushes can be performed by two methods[41], either grafting-to or grafting-from. Grafting to involves pre-synthesis of the polymer with a reactive terminal group to attach to the surface[42,43]. Pre-synthesis allows for direct control of properties of the polymer such as poly dispersity index and average molecular weight. Grafting-to also does not typically involve treatment of the surface before

functionalization for reactivity with the surface. This is often accomplished by mixing in monomers which diffuse to the surface or using a special catalyst to react with the surface. Grafting from does not involve pre-synthesis of the polymer[44], rather it involves using monomers and performing in situ polymerization to not only bond to the surface but also form the polymer chains. This technique does require pre-treatment of the surface unlike grafting to but allows for greater grafting density.

Covalent bonding is not the only available pathway for surface functionalization. There are examples that involve the use of ionic bonds instead to impart functionality. Successive ionic layer adsorption and desorption (SILAR) coatings[45] or layer by layer[46,47] deposition is one such ionic technique where sequential adsorption of alternating charged species is used to create stack of functional coatings via a dip coating system. It is critical that each step be followed by a washing step to create a surface that can support sequential reactions. This allows for layers as thin as 1 nm and can be layered as many times as is desired.

There are some derivatization techniques that do not fit in the blanket categories of being either organic or ionic processes. These techniques are quite uncommon and do not share features in common. This can include the use of a surface energy imbalance technique[48], where during the initial mixing of PDMS another molecule is added into the pre-polymer mixture. One example of this used perfluoroether allylamide as a filler molecule due to its low solubility with PDMS at room temperature. Despite low solubility, the terminal allyl groups allow for it to still be incorporated during polymerization. The key to the surface functionalization comes from the natural reptations experienced by the PDMS chains, where the surface energy interactions of the

perfluoroether and air are more favorable than the natural interface between PDMS and air. This more favorable energy interface encourages mobility of the perfluoro chains to the surface effectively functionalizing the surface of PDMS.

Another technique not classified as organic, or inorganic is sputter coating. Sputter coating is a physical vapor deposition (PVD) that is used to deposit either metals or metal oxides onto a desired substrate[49]. This is achieved by impacting the surface of the metal being transferred with an energized gas, such as argon, causing fragmentation of the metal. As traces of the metal are ejected from the surface, they can collide with the surface being functionalized. Sputter coating the surface of PDMS can be performed with different metals and metal oxides, such as gold[50]. Sputter coating allows for easy control of the deposited metal layer on the surface by controlling the time of the deposition procedure.

1.2 Heterogeneous Modifications: From Patterns to Gradients

The previously outlined techniques on their own all constitute homogenous methods of surface functionalization. Homogeneous surfaces often only elicit one response and are lacking the level of sophistication for their intended applications. Utilization of a surface patterning technique i.e., photolithography[51], masking[52], gradients[53], etc., allows for the creation of surfaces that experiences more complex surface environments by varying the chemistry from one portion of the surface to the next. Traditional photolithography[54] is a patterning technique where computer assisted designs (CAD) are used to selectively polymerize a layer of photoresist. Etching away the unpolymerized photoresist results in posts of photoresist left on the scaffold[55,56]. These can be used for reverse molding of PDMS to create topographical patterns or channels

used in microfluidic devices[57]. These topographically variable PDMS structures can be used for applications outside microfluidics[58], serving as masters for the creation of mimic masks or stamps for stamp patterning techniques.

Masking is one of the most basic patterns that can be accomplished on PDMS. Creation of masks is performed by placing a master, often made by photolithographic techniques, face down of an inert substrate, like a glass slide, and then depositing a photopolymer, such as poly (methyl acrylate), around the outside of the master. Since the master features topographical features this can create channels for capillary action to carry the photopolymer through the entire pattern this technique is referred to as micro molding in capillaries (MIMIC)[59]. Once the polymer has completely flowed into the structure polymerization is performed. Removal of the master leaves behind the mimic mask on the glass slide. This mask can be placed on the elastomer surface prior to one of the previously mentioned chemical modifications, such as oxidation, to selectively limit the reactions to portions of the surface not covered by the mask. Our group has done work like this using a TEM grid to selectively oxidize the surface of PDMS (Figure 1.1 A-C) [37]. Further derivatization of the surface could only be performed on segments of the surface that were available to the oxidation process (Figure 1.1 D). This resulted in generation of a PDMS surface that contained patterned regions functionalized with FITC leading to a surface that displayed a variable phosphorescent response (Figure 1.1 E-F).

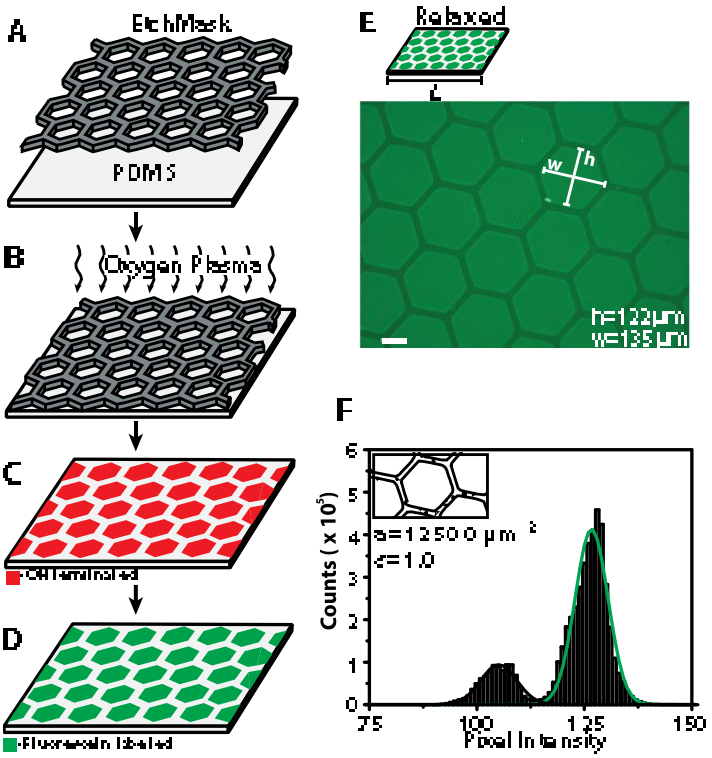

Figure 1.1 Schematic illustrating the masking and functionalization procedure. A) Application of the mask to a PDMS film. B) Selective oxidation of the exposed portions of the film. C) Patterned, silanol terminated portions of PDMS. D) functionalization of the surface with APTES and FITC yielding a selective fluorescein decorated surface. E) Fluorescence micrograph of a functionalized film. F) Pixel intensity histogram of the micrograph showed above. The green Gaussian curve measures intensity for hexagonal regions functionalized with FITC and the black Gaussian curve represents the native unfunctionalized PDMS. Scale bars represent 50 μm. Adapted with permission from reference 37.

A different approach to binary surface patterning is using micro-contact printing (μCP)[60]. In its simplest iteration μCP involves the use of a scaffold different from the surface that final functionalization is wanted on. Most of the critical functionalization steps take place on this separate substrate, referred to as a stamp[61]. Once the final functionalization has been performed the stamp is brought into contact with another surface and transfers the functionalization from the stamp to the new surface[62]. Due to the approaches taken with masking and μCP these techniques can yield inverse patterns of one another making both attractive prospects for patterned functionalization of PDMS surfaces. An advantage that μCP has over masking techniques is that since functionalization is performed on another substrate entirely, the stamps used can also be designed to be reusable[63].

While useful binary patterns are incredibly simple, capable of an on/off approach to functionality, and leave little room for nuance or further complexity in the pattern. Gradients are more complex patterns where a wide range of surface concentrations can be experienced in a comparatively small area which, in turn, can lead to more exotic responses not found through binary patterning approaches. Gradients can be formed on the surface of PDMS by several different methods. The most pervasive is a diffusion-based approach[64], where a silane is dissolved in a liquid with a high surface tension, often paraffin oil, and the mixture is then allowed to evaporate and slowly react across the surface (Figure 1.2 A-C). The concentration gradient that results from this gradual evaporation is imparted on the surface. The gradient intensity is easily tunable as well by simply allowing the silanization to occur for longer. Other methods for the formation of gradients include dip-coating[65], where the group of interest is dissolved in one layer while

another liquid, immiscible with the initial layer, is deposited on top of it and the group slowly diffuses into the recently added layer. This gradient of diffusion into the top layer is reflected in the sample dipped into this top layer creating a chemical gradient on the surface of the sample[66].

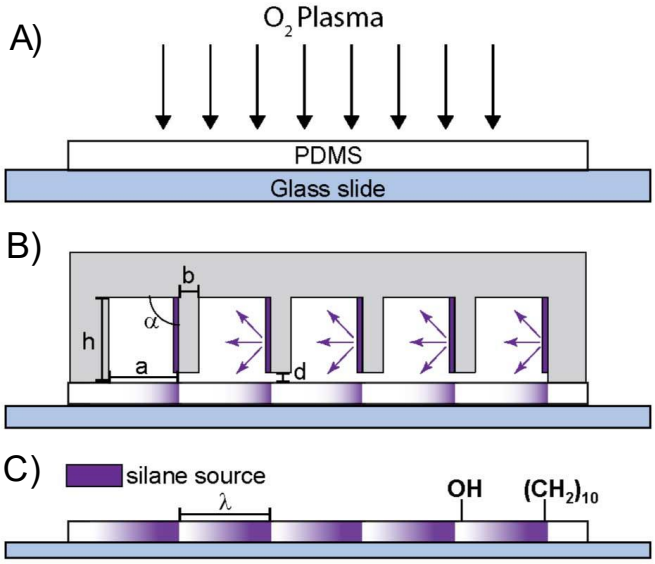

Figure 1.2 Illustration of diffusion based gradient generation A) oxidation of the surface of PDMS. B) Diffusion chamber for functionalization. The purple portions represent films soaked with a silane/oil mixture. C) Resultant surface with several gradients of identical intensity. Adapted with permission form reference 64.

1.3 Applications of Surface Chemical Modifications

Imparting new chemical functionality onto the surface of PDMS can create surfaces that behave vastly different from their native, unfunctionalized, counterparts. One example of this is the water surface contact angle. Native PDMS is a highly hydrophobic surface, with a contact angle of approximately 112°[67]. Performing one of the oxidation procedures already mentioned renders the surface hydrophilic, with a contact angle of approximately 7°. This large difference in the surface contact angle can be combined with a patterning technique, such as masking, to adjust the wettability of certain regions of the surface. The generation of these distinct regimes of hydrophilic or -phobic PDMS can be used for near instantaneous generation of large arrays of ordered liquid droplets (Figure 1.3 A-B). This was further confirmed by measuring the size distribution of the droplets on the surface (Figure 1.3 C-D). The idea of controlling wettability using chemistry and patterning can also be applied to gradient functionalized surfaces. Since gradients do not feature a harsh change in the wettability of the surface, this gentle change can instead be used for applications such as droplet motion. Whitesides[53] was one of the first to demonstrate this using a gradient of SAMs to make water run up an incline instead of flowing down it. Our group has also shown gradients generated on the surface of PDMS capable of droplet motion. This motion could also be controlled by varying the composition of the droplet with varying amounts of ethanol or ethylene glycol (Figure 1.3 E-F).

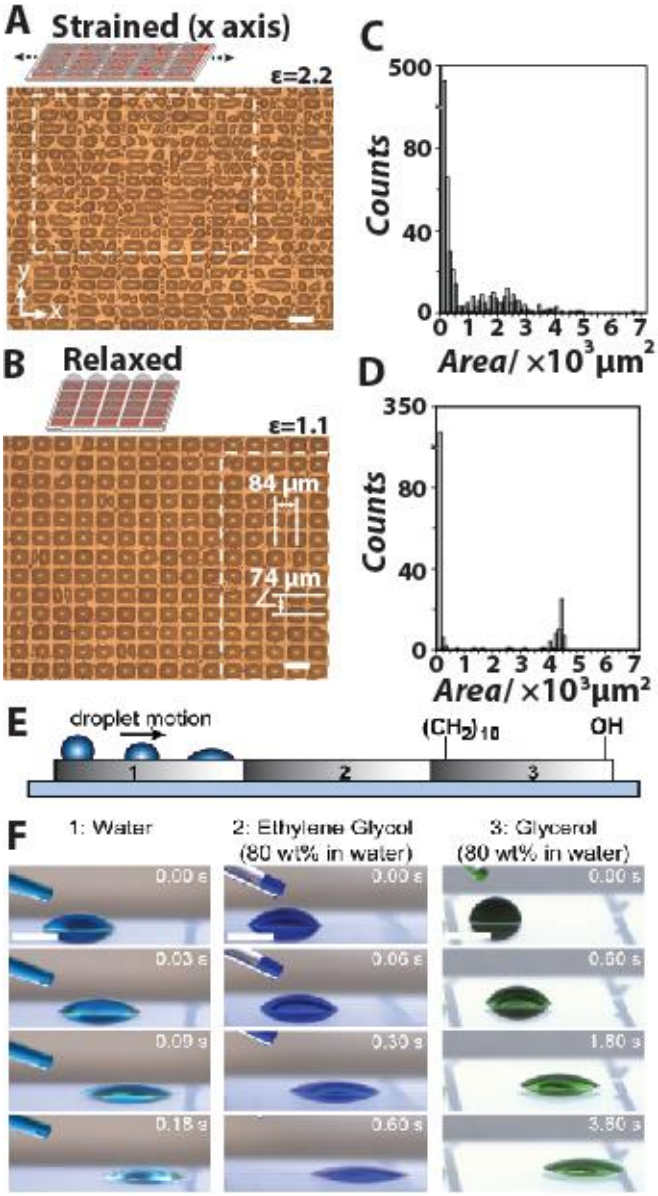

Figure 1.3 Patterning control of PDMS surface wettability. A) Optical micrograph of droplets nucleated on a strained and patterned surface. B) The same surface as A) after release of mechanical strain. C-D) histograms of droplet size distributions demonstrating a initial disorder state C) and assembly of the array D). E) illustration of droplets traveling across a chemical gradient. F) slow motion images of droplets with different compositions traveling across the surface of a chemical gradient. Adapted with permission from references 37 (A-D) and 64 (E-F).

Biomineralization is the process by which biological organisms can create complex and intricate hierarchical structures[68]. Despite the large amount of work done to understand this process synthetic systems remain unable to appreciably replicate these structures. One aspect that is well studied is the relationship between the nucleation rate and the relative surface energy of the nucleation site[69,70]. The biomineral calcium carbonate, $CaCO_3$, has attracted attention due to its ability nucleate and grow as several ordered structures, such as amorphous calcium carbonate, vaterite, aragonite, and calcite[71]. Some early work by Aizenberg[72] investigated how using simple chemical modifications, like SAMs, could direct calcium carbonate growth and nucleation. Several groups were used such as alcohols, carboxylic acids, phosphoric acids, sulphonic acids, and quaternary ammonium cations to probe what effect the terminal functional group might have on nucleation and growth. This work showed that groups such as the carboxylic acid or the sulphonic acid encouraged highly ordered growth of calcite on the surface and experienced nucleation orders of magnitude greater than surfaces left bare or functionalized with groups such as alcohols or alkyl terminal groups. This work was however limited to rigid surfaces featuring static chemical environments not often found in natural systems.

Soft materials, like silicone elastomers, present an opportunity to induce dynamic surface environments by utilizing their high yields points to subject the surface to successive strain cycling. The addition of strain also creates a difficult problem to overcome in the stark mechanical mismatch that the hard crystal and soft surface interface experiences. Our group[73] has worked on monitoring the adhesion of both zinc oxide (ZnO) and zinc hydroxysulfate (ZHS) by observing how ambient environment and

crystal morphology effected adhesion to the surface of PDMS. ZnO was deposited on the surface of patterned oxidized PDMS using a stamping procedure so that crystals were deposited across the entire surface (Figure 1.4 A). As PDMS was successively strained crystals remained adhered only on the native portions of PDMS. This closely mirrored Aizenberg's work where the growth of crystals was recorded higher on methylated surface compared to alcohol terminated surfaces (Figure 1.4 B-C). While important work for understanding how the changing surface environment of elastomeric materials effects the adhesion of crystal system this work did not involve the growth of crystals directly on the surface, instead choosing for pre-synthesis of crystals.

Going one step further and utilizing principles of dynamic surface attachment and chemical functionalization directed crystal growth, crystal growth on elastomers can be further modulated by creating surfaces featuring dynamic chemical environments. Using a simple surface derivatization technique, such as oxidation, the surface of PDMS can become incredibly high in relative surface energy creating an environment where calcium carbonate, $CaCO_3$, crystals do not grow (Figure 1.4 D). The native surface of PDMS, however has a much lower relative surface energy creating an environment where $CaCO_3$ growth is possible. Since oxidized PDMS is not a stable surface, it is possible to reconfigure the surface back to the native state by an application of strain, ε. This allows for creation of surfaces that can experience different relative surface energies as a function of the strain applied to the elastomer film (Figure 1.4 E-F). This was also combined with topographical features to vary the strain fields experienced by the surface and use topography to create regimes of varied surface energy

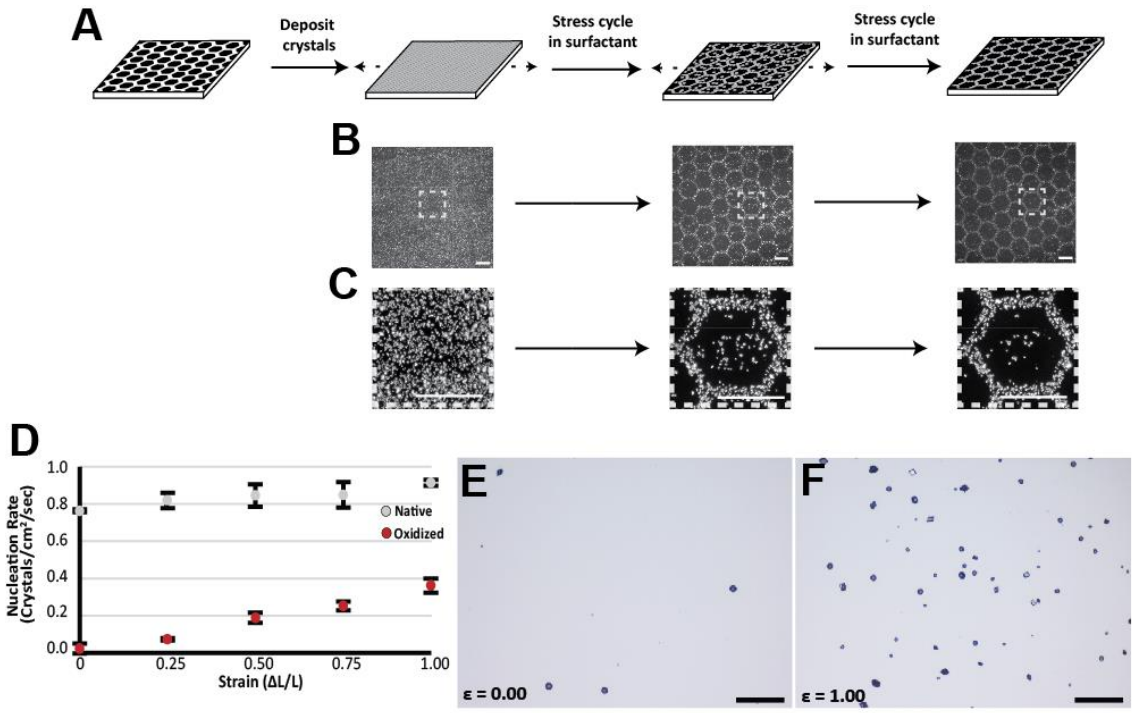

Figure 1.4 Crystal adhesion and growth on oxidized and native PDMS A) Illustration of how ZnO adherence to the surface of oxidized PDMS (black) and native PDMS (white). B) Left to right: PDMS surface immediately after deposition of ZnO crystals, after stress cycling the PDMS sample 1,500 times, and after stress cycling the PDMS sample 3,000 times. D) Graph plotting the relationship between nucleation rate and strain for native (gray) and oxidized (red) PDMS. E-F) optical micrographs of $CaCO_3$ grown on unstrained (E) and strained (F) surfaces of PDMS. Scale bars for B-C are 100 μm and for E-F are 200 μm. A-C) Adapted with permission from Rose, M.A.; Taylor, J.M.; Morin, S.A.; Adhesion of Morphologically Distinct Crystals to and Selective Release from Elastomeric Surfaces. Chem. Mater. 2016, 28 (23), 8513-8522. DOI: 10.1021/acs.chemmater.6b02575. Copyright 2021 American Chemical Society. D-F) Adapted with permission from reference 74.

.

Adhesion between two objects is a summation of several microscopic properties such as intermolecular forces, intramolecular bonds, and the area of contact between the two objects[75]. Decorating the surface of one or both objects involved in the adhesion with different functional groups can affect the adhesive forces they experience. One of the first examples of tuning the adhesion of PDMS is its use in microfluidic devices. Early generation microfluidic devices used special glass etching procedures to create the channels necessary for fluid transport. To reduce the time necessary to make microfluidic devices PDMS became an attractive prospect due to its use in replica molding[76]. Normally, PDMS experiences little adhesive force to the surface of glass, but if both surfaces are oxidized then their bonding becomes far greater. This led to PDMS becoming the standard for microfluidic devices due to ease of prototyping from replica molding and the rapid irreversible binding it experiences with glass. Inspired by this idea, our group has done work in creating all soft microfluidic devices by replacing the rigid glass support structure with a malleable commodity plastic like poly (ethylene terephthalate)[77], also known as PET. Functionalizing the surface of an oxidized commodity plastic with APTES resulted in only the amine terminated side binding to the surface. This resulted in a surface that had a free organo-silane end which could then be brought in contact with oxidized PDMS to create silyl ether bonds and establish irreversible covalent links between the two materials. The area where APTES bonded to plastic could also be patterned using reel-to-reel printing techniques. The areas patterned with printer inks would selectively block portions of the surface to being oxidized also preventing the binding of APTES. This was used to create all-soft microfluidic devices

whose design could be changed by printing a new design on PET, eliminating the need to lithographic techniques of 3-D printing new molds.

References

1. Hench, L. L.; Polak, J.M.; Third-Generation Biomedical Materials. *Science* **2002**, *295* (5557), 1014-1017. DOI: 10.1126/science.1067404
2. Chen, Q.; Liang, S.; Thouas, G. A.; Elastomeric Biomaterials for Tissue Engineering. *Progress in Polymer Science* **2013**, *38* (3-4), 584-671. DOI: 10.1016/j.progpolymsci.2012.05.003
3. Ko, H.; Javey, A.; Smart Actuators and Adhesives for Reconfigurable Matter. *Acc. Chem. Res.* **2017**, 50, 691−702. DOI: 10.1021/acs.accounts.6b00612
4. Guo, Q.; Chen, J.; Wang, J.; Zeng, H.; Yu, J.; Recent progress in the synthesis and application of mussel-inspired adhesives. *Nanoscale* **2020**, *12*, 1307-1324. DOI: 10.1039/C9NR09780E
5. Whitesides, G. M.; Soft Robotics. *Angew.Chem. Int. Ed.* **2018**, *57*,4258 –4273 DOI: 10.1002/anie.201800907
6. Polygerinos, P.; Correll, N.; Morin, S. A.; Mosadegh, B.; Onal, C. D.; Petersen, K.; Cianchetti, M.; Tolley, M. T.; Shepherd, R. F.; Soft Robotics: Review of Fluid-Driven Intrinsically Soft Devices; Manufacturing, Sensing, Control, and Applications in Human-Robot Interaction *ADVANCED ENGINEERING MATERIALS* **2017**, *19* (12), 1700016. DOI: 10.1002/adem.201700016
7. Thomsen, D. L.; Keller, P.; Naciri, J.; Jeon, H.; Shenoy, D.; Ratna, B. R.; Liquid Crystal Elastomers with Mechanical Properties of a Muscle. *Macromolecules* **2001**, *34*, 5868-5875. DOI: 10.1021/ma001639q
8. Zhang, W.; Gong, X.; Xuan, S.; Jiang, W.; Temperature-Dependent Mechanical Properties and Model of Magnetorheological Elastomers. *Ind. Eng. Chem. Res.* **2011**, *50*, 6704–6712 DOI: 10.1021/ie200386x
9. Hanzon, D. W.; Traugutt, N. A.; McBride M. K.; Bowman, C.N.; Yakacki, C. M.; Yu, K.; Adaptable Liquid Crystal Elastomers with Transesterification-based Bond Exchange Reactions. *Soft Matter*, **2018**, 14, 951-960. DOI: 10.1039/C7SM02110K
10. Jun, K.; Kim, D.; Ryu, S.; Oh, I.; Surface Modification of Anisotropic Dielectric Elastomer Actuators with Uni- and Bi-axially Wrinkled Carbon Electrodes for Wettability Control. *Scientific Reports*, **2017**, *7*, 6091. DOI: 10.1038/s41598-017-06274-0
11. Tang, M.; Zhang, R.; Li, S.; Zeng, J.; Luo, M.; Xu, Y.; Huang, G.; Towards a Supertough Thermoplastic Polyisoprene Elastomer Based on a Biomimic Strategy. *Angew. Chem.* **2018**, *130*, 16062 –16066. DOI: 10.1002/anie.201809339
12. Pei, A.; Malho, J.; Ruokolainen, J.; Zhou, Q.; Berglund, L. A.; Strong Nanocomposite Reinforcement Effects in Polyurethane Elastomer with Low Volume Fraction of Cellulose Nanocrystals. *Macromolecules*, **2011**, *44*, 4422–4427 DOI: 10.1021/ma200318k
13. Mazurek, P.; Vudayagiri, S.; Skov, A. L.; How to Tailor Flexible Silicone Elastomers with Mechanical Integrity: A Tutorial Review. *Chem. Soc. Rev.*, **2019**, *48*, 1448-1464. DOI: 10.1039/C8CS00963E
14. Johnston, I. D.; McCluskey, D. K.; Tan, C. K. L.; Tracey, M.C.; Mechanical Characterization of Bulk Sylgard 184 for Microfluidics and Microengineering. *J. Micromech. Microeng.*, **2014**, *24*, 035017.

15. Case. J. C.; White, E. L.; Kramer, R. K.; Soft Material Charaterization For Robotic Applications. *Soft Robotics*, **2015**, *2* (2). DOI: 10.1089/soro.2015.0002
16. Eduok, U.; Faye, O.; Szpunar, J.; Recent Developments and Applications of Protective Silicone Coatings: A Review of PDMS Functional Materials. *Progress in Organic Coatings*, **2017**, *111*, 124–163125. DOI: 10.1016/j.porgcoat.2017.05.012
17. Hong, S. M.; Kim, S. H.; Kim, J. H.; Hwang, H. I.; Hydrophilic Surface Modification of PDMS Using Atmospheric RF Plasma. *J. Phys.: Conf. Ser.*, **2006**, *34*, 108
18. Kim, Y. G.; Lim, N.; Kim, J.; Kim, C.; Lee, J.; Kwon, K.; Study on the Surface Energy Characteristics of Polydimethylsiloxane (PDMS) Films Modified by C_4F_8/O_2/Ar Plasma Treatment. *Applied Surface Science*, **2019**, *477*, 198–203 DOI: 10.1016/j.apsusc.2017.11.009
19. Yang, C.; Yuan, Y. J.; Investigation on the Mechanism of Nitrogen Plasma Modified PDMS Bonding with SU-8. *Applied Surface Science*, **2016**, *364*, 815–821 DOI: 0.1016/j.apsusc.2015.12.153
20. Bodas, D.; Khan-Malek, C.; Hydrophilization and Hydrophobic Recovery of PDMS by Oxygen Plasma and Chemical Treatment—An SEM Investigation. *Sensors and Actuators B*, **2007**, *123*, 368–373. DOI: 10.1016/j.snb.2006.08.037
21. Bèfahy, S.; Lipnik, P.; Pardoen, T.; Nascimento, C,; Patris, B.; Bertrand, P.; Yunus, S.; Thickness and Elastic Modulus of Plasma Treated PDMS Silica-like Surface Layer. *Langmuir*, **2010**, **26** (5), 3372–3375. DOI: 10.1021/la903154y
22. Kim, H. T.; Jeong, O. C.; PDMS Surface Modification using Atmospheric Pressure Plasma. *Microelectronic Engineering*, **2011**, *88* (8), 2281-2285. DOI: 10.1016/j.mee.2011.02.084
23. Brady, P. V.; Walther, J. V.; Kinetics of Quartz Dissolution at Low Temperatures. *Chemical Geology*, **1990**, *82*, 253-264. DOI: 10.1016/0009-2541(90)90084-K
24. Icenhower, J.P.; Dove, P. M.; The Dissolution Kinetics of Amorphous Silica into Sodium Chloride Solutions: Effects of Temperature and Ionic Strength. *Geochimica et Cosmochimica Acta*, **2000**, *64* (24), 4193-4203. DOI: 10.1016/S0016-7037(00)00487-7
25. Bilgin, S.; Isik, M.; Yilgor, E.; Yilgor, I.; Hydrophilization of Silicone-Urea Copolymer Surfaces by UV/ozone: Influence of PDMS Molecular Weight on Surface Oxidation and Hydrophobic Recovery. *Polymer*, **2013**, *54*, 6665-6675. DOI: 10.1016/j.polymer.2013.10.019
26. Atatde, D. de M.; Doi, I.; Highly Stable Hydrophilic Surfaces of PDMS Thin Layer Obtained by UV Radiation and Oxygen Plasma Treatments. *Physica Status Solidi C*, **2010**, *7* (2), 189-192. DOI: 10.1002/pssc.200982419
27. Morra, M.; Occhiello, E.; Garbassi, F.; Johnson, D.; On the Aging of Oxygen Plasma-Treated Polydimethylsiloxane Surfaces. *Journal of Colloid and Interface Science*, **1990**, *137* (1), 11-24. DOI: 10.1016/0021-9797(90)90038-P
28. Bain, C. D.; Evall, J.; Whitesides, G. M.; Formation of Monolayers by the Coadsorption of Thiols on Gold: Variation in the Head Group, Tail Group, and Solvent. *J. Am. Chem. Soc.*, **1989**, *111*, 7155-7164. DOI: 10.1021/ja00200a039
29. Poirier, G. E.; Pylant, E. D.; The Self-Assembly Mechanism of Alkanethiols on Au(111). *Science*, **1996**, *272* (5265), 1145-1148. DOI: 10.1126/science.272.5265.1145

30. Bain, C. D.; Whitesides, G. M.; Molecular-Level Control over Surface Order in Self-Assembled Monolayer Films of Thiols on Gold. *Science*, **1988**, *240* (4848), 62-63. DOI: 10.1126/science.240.4848.62
31. Sugimura, H.; Hozumi, A.; Kameyama, T.; Takai, O.; Organosilane Self-Assembled Monolayers Formed at the Vapour/Solid Interface. *Surface and Interface Analysis*, **2002**, *34* (1), 550-554. DOI: 10.1002/sia.1358
32. Hayashi, K.; Saito, N.; Sugimura, H.; Takai, O.; Nakagiri, N.; Regulation of the Surface Potential of Silicon Substrates in Micrometer Scale with Organosilane Self-Assembled Monolayers. *Langmuir*, **2002**, *18* (20), 7469-7472. DOI: 10.1021/la011707h
33. Zhou, J.; Khodakov, D. A.; Ellis, A. V.; Voelcker, N. H.; Surface Modification for PDMS-Based Microfluidic Devices. *Electrophoresis*, **2011**, *33* (1), 89-104. DOI: 10.1002/elps.201100482
34. Gelest, I., Silane Coupling Agents - Connecting Across Boundaries. In https://www.gelest.com/wp-content/uploads/Silane_Coupling_Agents.pdf, 2014; pp 1-71.
35. van Poll, M. L.; Khodabakhsh, S.; Brewer, P. J.; Shard, A.G.; Ramstedt, M.; Huck, W. T. S.; Surface Modification of PDMS *Via* Self-Organization of Vinyl-Terminated Small Molecules. *Soft Matter*, **2009**, *5*, 2286-2293. DOI: 10.1039/b901763a
36. Zhou, J.; Ellis, A. V.; Voeckler, N. H.; Recent Developments in PDMS Surface Modification for Microfluidic Devices. *Electrophoresis*, **2009**, *31* (1), 2-16. DOI: 10.1002/elps.200900475
37. Bowen, J. J.; Taylor, J. M.; Jurich, C. P.; Morin, S. A.; Stretchable Chemical Patterns for the Assembly and Manipulation of Arrays of Microdroplets with Lensing and Micromixing Functionality. *Adv. Funct. Mater*. **2015**, *25*, 5520–5528. DOI: 10.1002/adfm.201502174
38. Kuddannaya, S.; Chuah, Y. J.; Lee, M. H. A.; Menon, N. V.; Kang, Y.; Zhang, Y.; Surface Chemical Modification of Poly(dimethylsiloxane) for the Enhanced Adhesion and Proliferation of Mesenchymal Stem Cells. *ACS Appl. Mater. Interfaces*, **2013**, *5* (19), 9777-9784. DOI: 10.1021/am402903e
39. Zhao, X.; Kopelman, R.; Mechanism of Organosilane Self-Assembled Monolayer Formation on Silica Studied by Second-Harmonic Generation. *J. Phys. Chem.* **1996**, *100* (26), 11014–11018. DOI: 10.1021/jp9526657
40. Huang, H.; Chung, J. Y.; Nolte, A. J.; Stafford, C. M.; Characterizing Polymer Brushes via Surface Wrinkling. *Chem. Mater.* **2007**, *19* (26), 6555–6560. DOI: 10.1021/cm702456u
41. Sheparovych, R.; Motornov, M.; Minko, S.; Adapting Low-Adhesive Thin Films from Mixed Polymer Brushes. *Langmuir*, **2008**, *24* (24), 13828–13832. DOI: 10.1021/la803117y
42. Rubio, N.; Au, H.; Leese, H. S.; Hu,S.; Clancy, A. J.; Shaffer, M. P.; *Grafting from* versus *Grafting to* Approaches for the Functionalization of Graphene Nanoplatelets with Poly(methyl methacrylate). *Macromolecules*, **2017**, *50* (18), 7070–7079. DOI: 10.1021/acs.macromol.7b01047
43. Cordeiro, A. L.; Zschoche, S.; Janke, A.; Nitschke, M.; Werner, C.; Functionalization of Poly(dimethylsiloxane) Surfaces with Maleic Anhydride Copolymer Films. *Langmuir*, **2009**, *25*, 1509-1517. DOI: 10.1021/la803054s

44. Park, K. D.; Kim, Y. S.; Han, D. K.; Kim, Y. H.; Lee, E. H. B.; Suh, H.; Choi, K. S.; Bacterial Adhesion on PEG Modified Polyurethane Surfaces. *Biomaterials*, **1998**, *19*, 851— 859. DOI: 10.1016/S0142-9612(97)00245-7
45. Ghaleh, H.; Jalili, K.; Maher, B. M.; Rahbarghazi, R,; Mehrjoo, M.; Bonakdar, S.; Abbasi, F.; Biomimetic Antifouling PDMS Surface Developed Via Well-Defined Polymer Brushes for Cardiovascular Applications. *European Polymer Journal*, **2018**, *106*, 305-317. DOI: 10.1016/j.eurpolymj.2018.08.003
46. Chaki, S. H.; Chaudhury, M. D.; Deshpande, M. P.; SnS Thin Films Deposited by Chemical Bath Deposition, Dip Coating and SILAR Techniques. *Semicond.*, **2016**, *37* (5), 053001.
47. Mehta, G.; Kiel, M. J.; Lee, J. W.; Kotov, N.; Linderman, J. J.; Takayama, S.; Polyelectrolyte-Clay-Protein Layer Films on Microfluidic PDMS Bioreactor Surfaces for Primary Murine Bone Marrow Culture. *Adv. Funct. Mater*., **2007**, *17*, 2701–2709. DOI: 10.1002/adfm.200700016
48. Nolte, A. J.; Chung, J. Y.; Walker, M. L.; Stafford, C. M.; In situ Adhesion Measurements Utilizing Layer-by-Layer Functionalized Surfaces. *ACS Appl. Mater. & Inter.*, **2009,** *1* (2), 373-380. DOI: 10.1021/am8000874
49. Thanawala, S. K.; Chaudhury, M. K.; Surface Modification of Silicone Elastomer Using Perfluorinated Ether. *Langmuir*, **2000**, *16*, 1256-1260. DOI: 10.1021/la9906626
50. Thornton, J. A.; Sputter Coating— Its Principles and Potential. *SAE Transactions*, **1973**, 82 (3), 1787-1805.
51. Hassanin, H.; Mohammadkhani, A.; Jiang, K.; Fabrication of Hybrid Nanostructured Arrays Using a PDMS/PDMS Replication Process. *Lab Chip*, **2012**, *12*, 4160-4167. DOI: 10.1039/C2LC40512A
52. Francis, G.; Stuart, B. W.; Assender, H. E.; Selective Ozone Treatment of PDMS Printing Stamps for Selective Ag Metallization: A New Approach to Improving Resolution in Patterned Flexible/Stretchable Electronics. *Journal of Colloid and Interface Science*, **2020**, *568*, 273–281. DOI: 10.1016/j.jcis.2020.02.008
53. Chaudhury, M. K.; Whitesides, G. M.; How to Make Water Run Uphill. *Sciecne*, **1992**, *256* (5063), 1539-1541. DOI: 10.1126/science.256.5063.1539
54. Seisyan, R. P.; Nanolithography in Microelectronics: A Review. *Technical Physics*, **2011**, *56* (8), 1061-1073. DOI: 10.1134/S1063784211080214
55. Chen, W.; Lam, R. H. W.; Fu, J.; Photolithographic Surface Micromachining of Polydimethylsiloxane (PDMS). *Lab Chip*, **2012**, *12*, 391-395. DOI: 10.1039/C1LC20721K
56. Li, C.; Cheung, C. N.; Yang, J.; Tzang, C. H.; Yang, M.; PDMS-Based Microfluidic Device with Multi-Height Structures Fabricated by Single-Step Photolithography using Printed Circuit Board as Masters. *Analyst*, **2003**, *128*, 1137-1142. DOI: 10.1039/B304354A
57. Kim, K.; Park, S.; Lee, J.-B.; Manohara, H.; Murphy, M.; Ahn, C. H.; Rapid Replication of Polymeric and Metallic High Aspect Ratio Microstructures using PDMS and LIGA Technology. *Microsystem Technologies*, **2002**, *9*, 5–10. DOI: 10.1007/s00542-002-0194-6
58. Getu, H.; Spelt, J. K.; Papini, M.; Thermal Analysis of Cryogenically Assisted Abrasive Jet Micromachining of PDMS. *International Journal of Machine Tools & Manufacture*, 2011, *51*, 721–730. DOI: 10.1016/j.ijmachtools.2011.05.003

59. E. Kim, Y. Xia, and G.M. Whitesides: Polymer Microstructures Formed by Molding in Capillaries. *Nature* **1995**, *376*, 581-584. DOI: 10.1038/376581a0
60. Perl, A.; Reinhoudt, D. N.; Huskens, J.; Microcontact Printing: Limitations and Achievements. *Adv. Mater*., **2009**, *21*, 2257–2268. DOI:10.1002/adma.200801864
61. Ruiz, S. A.; Chen, C.S.; Microcontact printing: A tool to pattern. *Soft Matter*, **2007**, *3*, 168–177. DOI: 10.1039/b613349e
62. Liu, C.-X.; Choi, J.-W.; Patterning Conductive PDMS Nanocomposite in an Elastomer using Microcontact Printing. *J. Micromech. Microeng.*, **2009**, *19*, 085019
63. Csucs, G.; Künzler, T.; Feldman, K.; Robin, F.; Spencer, N. D.; Microcontact Printing of Macromolecules with Submicrometer Resolution by Means of Polyolefin Stamps. *Langmuir* **2003**, *19* (15), 6104–6109. DOI: 10.1021/la0342823
64. Perex-Toralla, K.; Konda, A.; Bowen, J. J.; Jennings, E.; Argyropoulos, C.; Morin, S. A.; Rational Synthesis of Large-Area Periodic Chemical Gradients for the Manipulation of Liquid Droplets and Gas Bubbles. *Advanc. Funct. Mater.*, **2018**, *28* (8), 1705564. DOI: 10.1002/adfm.201705564
65. Faustini, M.; Ceratti, D. R.; Louis, B.; Boudot, M.; Albouy, P.-A.; Boissière, C.; Grosso, D.; Engineering Functionality Gradients by Dip Coating Process in Acceleration Mode. *ACS Appl. Mater. Interfaces* **2014**, *6* (19), 17102–17110. DOI: 10.1021/am504770x
66. Kim, M.; Song, K. H.; Doh, J.; PDMS Bonding to a Bio-Friendly Photoresist via Self-Polymerized Poly(dopamine) Adhesive for Complex Protein Micropatterning Inside Microfluidic Channels. *Colloids and Surfaces B: Biointerfaces*, **2013**, *112*, 134–138. DOI: 10.1016/j.colsurfb.2013.07.021
67. Hillborg, H.; Gedde, U. W.; Hydrophobicity Recovery of Polydimethylsiloxane After Exposure to Corona Discharges. *Polymer*, **1998**, *39*, 1991-1998. DOI: 10.1016/S0032-3861(97)00484-9
68. Mann, S.; Molecular Recognition in Biomineralization. *Nature*, **1988**, *322*, 119-124. DOI: 10.1038/332119a0
69. Smeets, P. J. M.; Cho, K. R.; Kempen, R. G. E.; Sommerdijk, N. A. J. M.; Yoreo, J. J.; Calcium Carbonate Nucleation Driven by Ion Binding in a Biomimetic Matrix Revealed by *In situ* Electron Microscopy. *Nature Materials*, **2015**, *14*, 394-399. DOI: 10.1038/NMAT4193
70. Markov, I. V. *Crystal growth for Beginners: Fundamentals of Nucleation, Crystal Growth and Epitaxy*, World Scientific, Singapore, River Edge, N.J., 2003. DOI: 10.2113/0540057
71. Dhami, N. K.; Reddy, M. S.; Mukherjee A.; Biomineralization of Calcium Carbonates and their Engineered Applications: A Review. *Front. Mirobiol.*, **2013**, *4*, 314. DOI: 10.3389/fmicb.2013.00314
72. Aizenberg, J.; Black, A. J.; Whitesides, G. M.; Oriented Growth of Calcite Controlled by Self-Assembled Monolayers of Functionalized Alkanethiols Supported on Gold and Silver. *J. Am. Chem. Soc.* **1999**, *121* (18), 4500–4509. DOI: 10.1021/ja984254k
73. Rose, M.A.; Taylor, J.M.; Morin, S.A.; Adhesion of Morphologically Distinct Crystals to and Selective Release from Elastomeric Surfaces. *Chem. Mater*. **2016**, *28* (23), 8513-8522. DOI: 10.1021/acs.chemmater.6b02575

74. Taylor, J.M.; Konda, A.; Morin, S.A.; Spatiotemporal Control of Calcium Carbonate Nucleation Using Programmable Deformations of Elastic Surfaces. *Soft Matter* **2020**, *16*, 6038-6043. DOI: 10.1039/d0sm00734j
75. Götzinger, M.; Peukert, W.; Particle Adhesion Force Distributions on Rough Surfaces. *Langmuir* **2004**, *20* (13), 5298–5303. DOI: 10.1021/la049914f
76. Sia, S. K.; Whitesides, B. M.; Microfluidic Devices Fabricated in Poly(dimethylsiloxane) for Biological Studies. *Electrophoresis*, **2003**, *24*, 3563–3576. DOI: 10**.**1002/elps**.**200305584
77. Taylor, J.M., Perez-Toralla; K., Aispuro, R.; Morin, S.A.; Covalent Bonding of Thermoplastics to Rubbers for Printable, Reel-to-Reel Processing in Soft Robotics and Microfluidics *Adv. Mater.*, **2018**, *30*, 1705333. DOI: 10.1002/adma.201705333

CHAPTER 2: ORGANIC REACTIONS TO EXPAND THE SCOPE OF ORGANO-SILANE FUNCTIONAL GROUPS

2.1 Click Chemistry on PDMS surfaces

Despite the pervasiveness of SAMs[1,2] and organo-silanes[3,4] towards functionalization of the surface of silicone elastomers, the required formation of silyl ethers precludes the use of several functional groups including alcohols and carboxylic acids. Efforts to try and rectify this involve functionalization using silanes with reactive functional groups. This allows functionalization to continue after formation of SAMs or grafting of polymers to or from the surface. A straightforward utilization of this idea is to use simple organic reactions to increase the scope of surface functional reactions available on PDMS[5,6]. To accomplish this the reactions used must be performable in media compatible with PDMS, be performed at a relatively low temperature, and utilize robust reagents that are stable under ambient conditions.

The click family of reactions has already seen some applications for fulfilling these criteria. The term “click chemistry” is attributed primarily to K. Barry Sharpless[7], who coined the name in a paper discussing the need for more green chemical reactions. In the same breath, he also describes several properties a reaction should possess to be considered a click reaction. This includes an overall negative demand in free energy, use of environmentally friendly solvents, wide reactive scope, high yield, easily isolated products, and high stereospecificity. After this, two reactions specifically became exemplars to represent click reactions as a whole: the thiol-ene reaction[8,9] and 1,3-triazole ring formation[10]. Triazole ring formation can also be sub-divided into two distinct

mechanistic pathways: the copper-catalyzed azide alkyne click reaction (CuAAC)[11] and the copper-free azide alkyne click reaction (SPAAC)[12].

The SPAAC reaction, while not requiring the use a metal catalyst, is the less common of the two mechanistic pathways. This is because the number of useable alkynes for this reaction are much more limited than the copper-catalyzed reaction. The SPAAC reaction requires the use of cyclooctynes[13], due to their high internal steric strain. This large strain is alleviated during the transition to the triazole ring and helps to provide much of the negative energy demand for the reaction to proceed. The CuAAC reaction involves complexation of the alkyne to a copper (I) catalyst[14]. This complexation results in the formation a reactive alkyne species that can further react with the azide group to form the triazole ring. Due to the complexation step, the scope of this reaction is essentially only limited to the number of available alkynes and azides. This large scope was the driving factor behind choosing the CuAAC reaction.

PDMS, Sylgard 184, was prepared according to manufacturer instructions in a 10:1 (monomer: catalyst) ratio, stirred, and degassed under vacuum. After degassing, the polymer mixture was poured onto a clean silica wafer and scraped to a uniform thickness of 500 μm using a Zehntner manual film applicator. The PDMS was then placed in a 60°C oven for 2 hours to completely cure the polymer. The PDMS was then cut into 1cm x 3 cm strips which served as the scaffold for surface functionalization and subsequent applications. Oxidation was conducted on the strips using a PlasmaEtch system set to 10% power for 10 seconds. This rendered the surface completely hydrophilic but did not create a very thick silica layer.

After oxidation was silanization, which was performed by placing the strips on a hot plate at 150°C adjacent to 0.5 mL of 11-bromoundecyl trichlorosilane. The entire system was covered using a glass dish and the silanization process was completed in 5 minutes. After silanization, a substitution reaction was required to replace the terminal halide with an azide group. This was accomplished by submerging the silanized sample in a mixture of 125 mg sodium azide (NaN_3) in 20 mL of N,N-Dimethyl formamide (DMF) for 1 hour. After submersion, the surface was rinsed with acetone and dried with N_2 gas to remove unreacted reagents from the surface.

After the substitution reaction the surface is primed for the click reaction. The click reaction was performed by creating a mixture of 25 mg of copper (II) sulfate, 59.5 mg of sodium (L)-ascorbate, and 0.17 μmol of whichever alkyne is being used in the reaction in 18 MΩ water. The creation of the copper-alkyne complex was easy to see visually, with the addition of the alkyne immediately changing the color of mixture from bright orange to a yellow or brown depending on the alkyne. The reaction was performed over the course of 1 hr with gentle stirring, after which samples were removed from the reaction vessel, rinsed with de-ionized water, and dried with N_2 gas to remove excess reagent from the surface (Figure 2.1 A).

2.1.1 Characterization

Characterization of the surface was performed using X-ray photoelectron spectroscopy (XPS) and surface contact angle. XPS allows for probing of the surface environment qualitatively and quantitatively by scanning for different elements and relating the relative peak intensity to the surface concentration of the group. With the penetration depth of XPS being approximately 1 nm it is incredibly useful for surface

level elemental composition. Using contact angle alongside XPS allows for probing of the relative surface energy and how it varies during different stages of the functionalization process. Contact angle was performed using a Biolin Scientific Theta OneAttension with 5 μL droplets deposited onto the surface. Contact angles were reported as an average of three different positions for samples prepared homogeneously. Combining these techniques shows how the reactions change the surface environment from one step to another and eventually decorate the surface with desired functional groups such as carboxylic acids.

2.1.2 Results & Discussion

Since the functionalization of the surface was not a one-step process, elements can be added and removed from the surface following different steps. This proved useful as the presence, or lack thereof, of certain elements was expected given the purpose each step of the process is meant to accomplish. Bromine specifically, was included in the initial silanization step with the express purpose of serving as a sacrificial group to allow for binding of the azide to the surface, leading to a strong XPS signal initially and then little to no signal after subsequent steps are performed (Figure 2.1 B). Nitrogen on the other hand was not present for initial silanization step, reflected in no XPS signal at first, but after the substitution step there is a small peak that becomes much larger following the click reaction (Figure 2.1 C). Finally, phosphorous was not exposed to the surface until the click chemistry step, so the lack of a strong phosphorous peak indicates the success of the click chemistry reaction using even a sterically bulky triphenyl phosphine group (Figure 2.1 D).

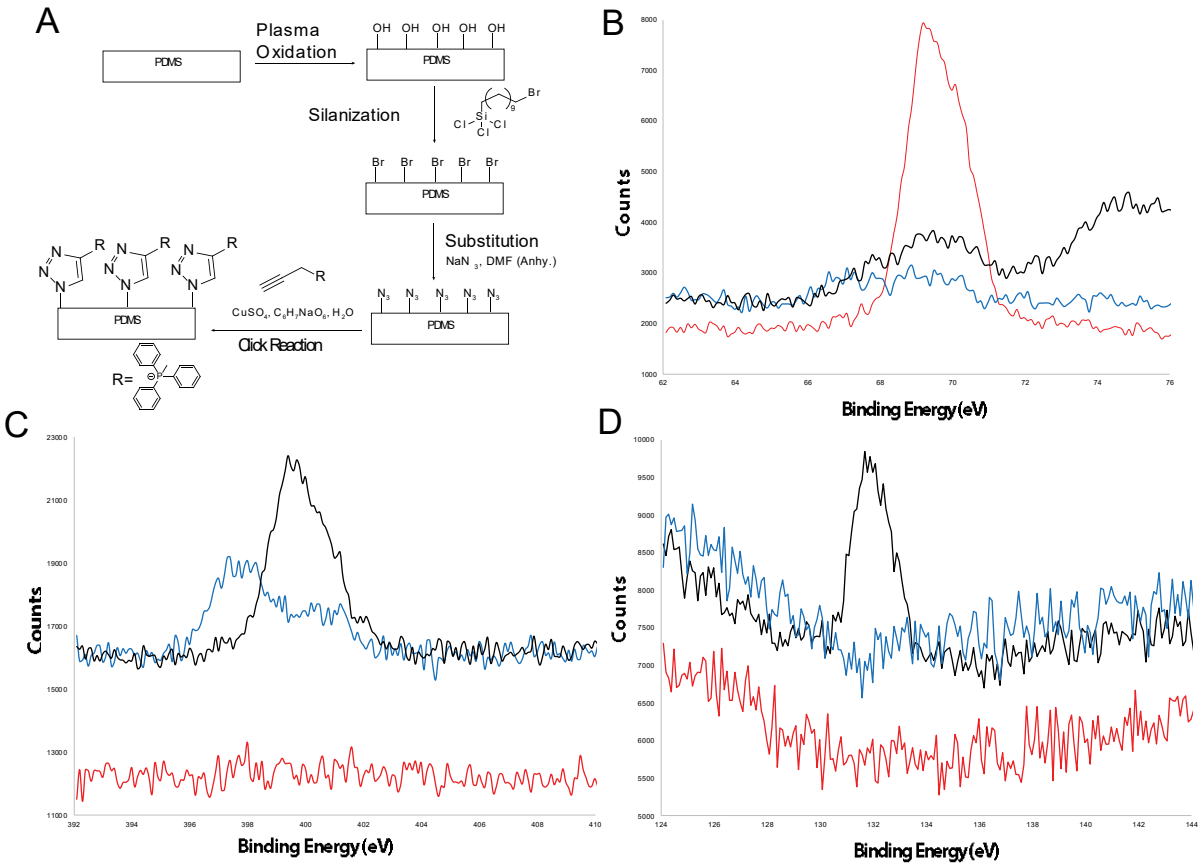

Figure 2.1 XPS data demonstrating surface functionalization using click chemistry A) Illustration of the functionalization of PDMS. B) XPS scans for the presence of bromine after silanization (red), substitution (blue), and the click reaction (black). C) XPS scans for the presence of nitrogen after silanization (red), substitution (blue), and the click reaction (black). D) XPS scans for the presence of phosphorous after silanization (red), substitution (blue), and the click reaction (black).

Despite the presence of phosphorous being undetected until the click reaction is performed there is still the possibility of intermolecular forces contributing to non-specific adsorption to the surface. To confirm the success of the click reaction the original reaction scheme was tested against a chemically similar reaction set-up that is known to not perform the reaction. For the click reaction to effectively proceed a specific complexation between copper and the alkyne. This complexation requires the presence of free copper (I) ions. Copper (I) salts, like CuCl, despite containing of the correct copper species do not sufficiently dissociate in water and cannot serve as a source of catalytic copper for the CuAAC reaction. Using this fact, non-specific adsorption and the success of the click reaction was tested by performing the CuAAC reaction as normal and while changing the catalyst from $CuSO_4$ to CuCl. When the CuAAC reaction was conducted normally the phosphorous peak was once again observed and was stable to submersion in water, with mild agitation, for at least 10 minutes (Figure 2.2 A). Meanwhile, when the catalyst was changed to CuCl, there was a strong initial phosphorous, like the standard catalyst, but this surface was much less stable. As the surface was washed using the same conditions as the standard procedure there is a drastic decrease in the phosphorous peak, with almost all the phosphorous washed away from the surface by 10 minutes (Figure 2.2 B).

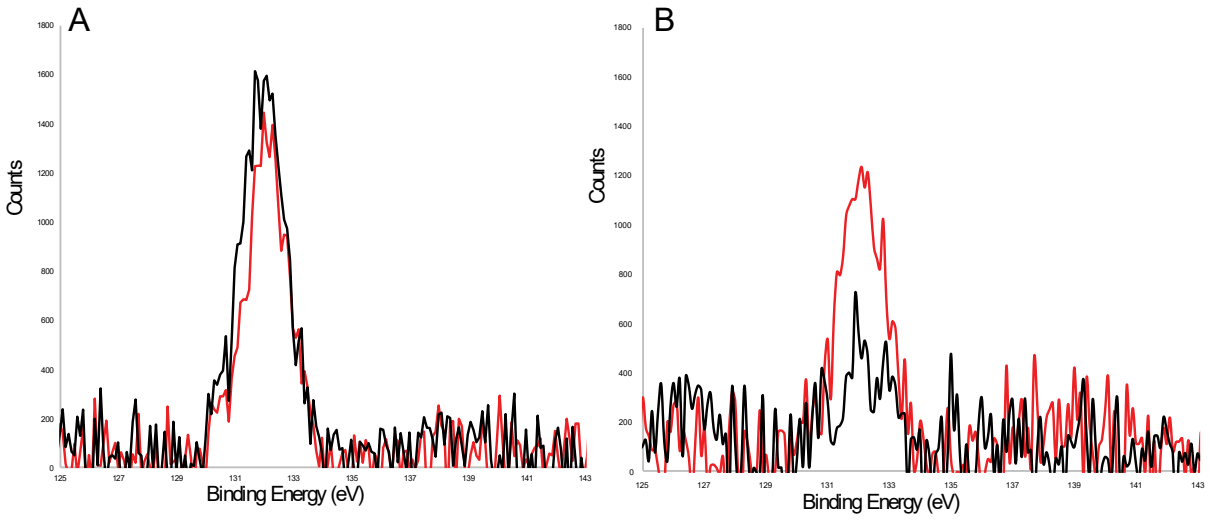

Figure 2.2 Surface composition comparison between copper catalysts. A) Phosphorous XPS elemental scans for surfaces functionaluzed using $CuSO_4$ catalyst and washed for 5 minutes (red) and 10 minutes (black). B) Phosphorous XPS elemental scans for surfaces functionalized using CuBr catalyst and washed for 5 minutes (red) and 10 minutes (black).

As mentioned previously, one of the greatest advantages of functionalizing PDMS surfaces with the click reaction is the large scope of reactants available for use. Groups such an aromatic thiophene ring and functional groups unavailable by conventional organo-silane methods can functionalize the surface. Measuring the presence of the thiophene ring was the same as measuring for the triphenyl phosphine, except the scan was for sulfur instead of phosphorous. The thiophene ring was also stable on the surface when washed with water for 5 minutes. When the wash time was increased to 10 minutes there was a decrease in the peak but not to the same degree as the copper halide catalyzed samples. This decrease in peak intensity could be attributed to variations in concentration across the surface (Figure 2.3 A). Measuring the success of functional groups like carboxylic acids and alcohols proves a more difficult task than thiophene rings or triphenyl phosphines.

Without the introduction of new elements to the surface, by the click reaction, XPS proves a less effective characterization technique. In these instances, surface contact angle was used to approximate the relative surface energy and how the attachment of these different functional groups effects that. Each step of the functionalization process produced a surface contact angel distinct from the step preceding it. When the click reaction was performed using propargyl alcohol as the alkyne the contact angle approached that of oxidized surfaces. Considering this functionalized the surface with alcohol groups it was a positive sign the reaction succeeded. When propiolic acid, to functionalize with carboxylic acids, was used as the alkyne the contact angle decreased again but not as much alcohol functionalized surfaces (Figure 2.3 B).

A

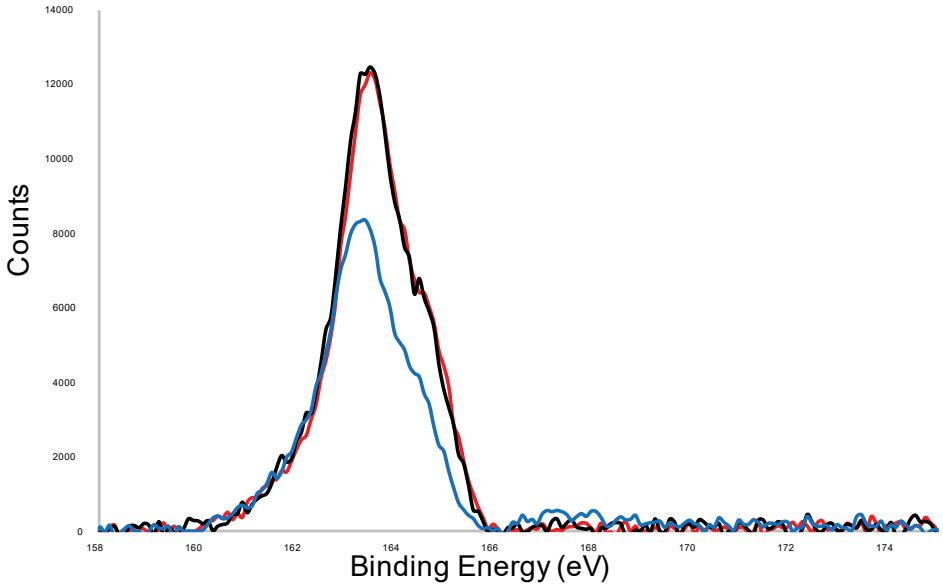

B

Functionalization	Native	Oxidation	Silanization	Azide Subsitution	Click Reaction COOH	Click Reaction COH
Contact Angle (± STD) with Water	117.71±0.06	2.05±1.55	87.29±4.21	97.29±10.98	57.49±2.92	41.49±4.25

Figure 2.3 Surface click reaction scope study A) Sulfur XPS elemental scans for a thiophene functionalized surface (red) and washed for 5 minutes (black) and 10 minutes (blue). B) Table of surface contact angles for each step of the functionalization process.

2.2 Kirigami Inspired Smart Adhesive Composite

Modern adhesives utilize a homogeneous adhesive surface resulting in an equal amount of force required for delamination regardless of the release axis. Creation of materials that feature a preferential delamination direction, a quick release axis, is important for the creation of materials designed to be temporarily adhered. Work to try and program a quick release axi is focused on only the design and shape of the vessel with adhesive properties[15]. This has been done with kirigami, the ancient Japanese art of paper cutting, to create a non-conformally contacted interface and decreasing the adhesive area[16]. When the kirigami is performed selectively with gaps favoring one axis over another it can create a difference in the delamination force profile for one direction over another. While promising, kirigami alone does not produce enough of a force difference for one axis of release over another.

Kirigami only limits the adhesive forces by controlling the contact area for adhesion. Another major aspect of adhesion is the chemical groups giving rise to the adhesive forces. Adding directionality to the chemistry of adhesion should allow for more control of the directionality of delamination. Our group has already shown a simple method using reel to reel printing techniques to pattern the adhesion experienced between PDMS and commercial plastics[17]. Combining the principals of kirigami to limit contact area and chemical patterning to limit chemical adhesion should allow for more fine-tuned control of the delamination of commercial plastics from PDMS.

2.2.1 Methods

Poly (ethylene terephthalate) ((PET)) sheets were purchased as slide transparencies from an office supplies retailer. The sheets were then cut into a 5x8 inch rectangles and washed by ultrasonication in toluene, isopropyl alcohol, and then water for 5 minutes each. After washing and drying, the sheets were placed into an HP Laserjet® m551 color printer where designs were printed onto the sheets (Figure 2.4 A-B). Next a Cricut® craft cutter was used to create the kirigami pattern by selectively cutting out pre-determined parts of the pattern (Figure 2.4 C). This yielded sheets 1.8 inches wide by 7.5 inches long with kirigami cut outs and patterns for selective functionalization on the surface. The samples were this long to allow for multiple spaces with patterned functionalization.

PDMS was prepared according to manufacturer specifications by mixing creating a mixture of 10:1 (w/w) monomer to catalyst and stirring completely. The mixture was then degassed by vacuum until all air bubbles were removed from the mixture. Then the mixture was poured into a mold to achieve dimensions of 3 cm x 10 cm x 2 cm. Once the mold was filled it was transferred to a 60°C oven and cured for 2 hours. After curing the PDMS was demolded and transferred to a clean glass slab for oxidation and composite assembly.

PDMS was simply oxidized using a PlasmaEtch system at 60% power for 30 seconds to completely oxidize the surface (Figure 2.4 F). Functionalization of the PET sheets was conducted by using UVO followed by a liquid deposition of the adhesive compound onto the surface. UVO was conducted using a UV lamp for 1 minute to selectively oxidize the surface. The success of this step was determined qualitatively by using a water droplet and observing the wettability on surfaces printed with ink and

oxidized surfaces. After confirming the oxidation, the strip was dropped in a pre-prepared solution of poly (ethylene imine), or PEI, in water (Figure 2.4 D-E). To achieve complete dissolution of PEI the solution was heated to 60°C and was used hot to avoid PEI crashing back out of solution. PEI was used to create this composite due to its lack of formal bonds with oxidized PDMS. Relying on the hydrogen bonding experienced between the two surfaces results in one that is reversibly adhered compared to previous work that was concerned with creating irreversible bonds. After functionalization of the PET sheets and oxidation of the PDMS slab was completed, the composite was assembled by placing the functionalized side of the PET sheet onto the oxidized surface of PDMS (Figure 2.4 G). The PET sheet was smoothed out onto the PDMS to ensure complete conformal contact between the two surfaces. The composite was then weighed down and left to sit overnight to achieve maximum adhesion on the surface.

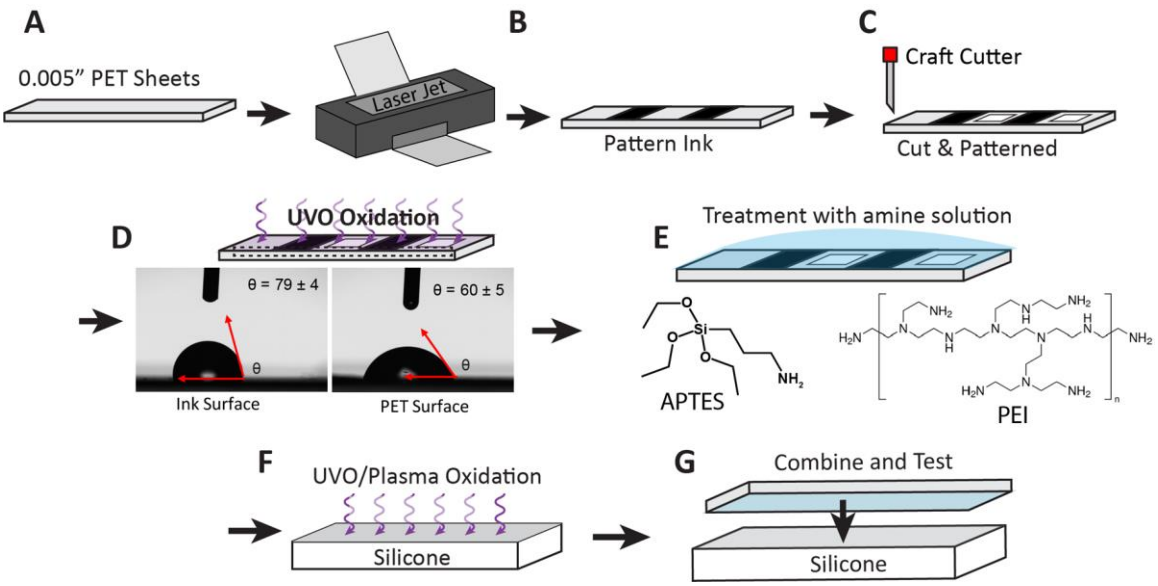

Figure 2.4 Illustration of Kirigami composite assembly A-B) Cleaning and printing of patterns onto PET sheets. C) Removal of pre-determined portions of PET to create a kirigami design. D) UVO treatment of printed and cut PET samples, images included are surface contact angle measurements of ink printed (left) and bare (right) PET after UVO. E) Chemical treatment of the oxidized PET surface with PEI. F-G) Oxidation of PDMS (F) and then assembly of composite material (G).

References

1. Ferguson, G.S.; Chaudhury, M. K.; Biebuyck, H. A.; Whitesides, G. M.; Monolayers on Disordered Substrates: Self-Assembly of Alkyltrichlorosilanes on Surface Modified Polyethylene and Poly(dimethylsiloxane). *Macromolecules* **1993**, *26*, 5870-5875. DOI: 10.1021/ma00074a007
2. Chaudhury, M. K.; Self-Assembled Monolayers on Polymer Surfaces. *Biosensors and Bioelectronics*, **1995**, *10 (9)*, 785-788. DOI: 10.1016/0956-5663(95)99216-8
3. Lee, K. S.; Ram, R. J.; Plastic–PDMS Bonding for High Pressure Hydrolytically Stable Active Microfluidics. *Lab Chip*, **2009**, *9*, 1618-1624. DOI: 10.1039/B820924C
4. Lu, N.; Zhang, W.; Weng, Y.; Chen, X.; Cheng, Y.; Zhou, P.; Fabrication of PDMS Surfaces with Micro Patterns and the effect of Pattern Sizes on Bacteria Adhesion. *Food Control*, **2016**, *68*, 344-351. DOI: 10.1016/j.foodcont.2016.04.014
5. Zhang, J.; Chen, Y.; Brook, M. A.; Facile Functionalization of PDMS Elastomer Surfaces Using Thiol–Ene Click Chemistry. *Langmuir*, **2013**, *29* (40), 12432–12442. DOI: 10.1021/la403425d
6. Zhang, Z.; Feng, X.; Xu, F.; Liu, X.; Liu, B.-F.; "Click" Chemistry-Based Surface Modification of Poly(dimethylsiloxane) for Protein Separation in a Microfluidic Chip. *Electrophoresis*, **2010**, *31* (18), 3129-3136. DOI: 10.1002/elps.201000208
7. Kolb, H. C.; Finn, M. G.; Sharpless, K. B.; Click Chemistry: Diverse Chemical Function from a Few Good Reactions. *Ange. Chem. Int. Ed.*, **2001**, *40* (11), 2004-2021. DOI: 10.1002/1521-3773(20010601)40:11<2004::AID-ANIE2004>3.0.CO;2-5
8. Hoyle, C. E.; Bowman, C. N.; Thiol–Ene Click Chemistry. *Ange. Chem. Int. Ed.*, **2010**, *49* (9), 1540-1573. DOI: 10.1002/anie.200903924
9. Rissing, C.; Son, D. Y.; Thiol−Ene Reaction for the Synthesis of Multifunctional Branched Organosilanes. *Organometallics*, **2008**, *27* (20), 5394–5397. DOI: 10.1021/om8003527
10. Fleming, D. A.; Thode, C.J.; Williams, M. E.; Triazole Cycloaddition as a General Route for Functionalization of Au Nanoparticles. *Chem. Mater.* **2006**, *18* (9), 2327–2334. DOI: 10.1021/cm060157b
11. Hein, J. E.; Fokin, V. V.; Copper-Catalyzed Azide–Alkyne Cycloaddition (CuAAC) and Beyond: New Reactivity of Copper(I) Acetylides. *Chem. Soc. Rev.*, **2010**, *39*, 1302-1315. DOI: 10.1039/B904091A
12. Mbua, N. E.; Guo, J.; Wolfert, M. A.; Steet R.; Boons G.-J.; Strain-Promoted Alkyne–Azide Cycloadditions (SPAAC) Reveal New Features of Glycoconjugate Biosynthesis. *ChemBioChem*, **2011**, *12* (12), 1912-1921. DOI: 10.1002/cbic.201100117
13. Dommerholt, J.; van Roojien, O.; Borrmann, A.; Guerra C. F.; Bickelhaupt, F. M.; van Delft, F. L.; Highly Accelerated Inverse Electron-Demand Cycloaddition of Electron-Deficient Azides with Aliphatic Cyclooctynes. *Nature Communications*, **2014**, *5*, 5378. DOI: 10.1038/ncomms6378
14. Liang, L.; Astruc, D.; The Copper(I)-Catalyzed Alkyne-Azide Cycloaddition (CuAAC) "Click" Reaction and its Applications. An Overview. *Coordination Chemistry Reviews*, **2011**, *255* (23), 2933-2945. DOI: 10.1016/j.ccr.2011.06.028

15. Hwang, D.-G.; Trent,K.; Bartlett, M.D.; Kirigami-Inspired Structures for Smart Adhesion. *ACS Appl. Mater. Interfaces*, **2018**, *10* (7), 6747–6754. DOI: 10.1021/acsami.7b18594
16. Zhao, R.; Lin, S.; Yuk, H.; Zhao, X.; Kirigami Enhances Film Adhesion. *Soft Matter*, **2018**, *14*, 2515-2525. DOI: 10.1039/C7SM02338C
17. Taylor, J.M., Perez-Toralla; K., Aispuro, R.; Morin, S.A.: Covalent Bonding of Thermoplastics to Rubbers for Printable, Reel-to-Reel Processing in Soft Robotics and Microfluidics *Adv. Mater.*, **2018**, *30*, 1705333. DOI: 10.1002/adma.201705333

CHAPTER 3: BIOMINERALIZATION AND PATTERNED ADHESION ON FUNCTIONALIZED PDMS SURFACES

3.1 Biomineralization on Click Functionalized Surfaces

In classical nucleation theory, heterogeneous nucleation is largely determined by the surface energy of interactions between the surface, solution, and crystal. Eq. 1 represents the relationship between the steady state nucleation rate (J_0) and the thermodynamic barrier for nucleation (ΔG^*)[1-3].

$$J_0 = Ae^{-(\Delta G^*)/k_B T} \qquad \text{Eq 3.1}$$

A represents a pre-exponential factor specific to the crystal and surface, k_B is the Boltzmann Constant and *T* is the absolute temperature. The thermodynamic barrier for nucleation can also be related to the net surface energy of the surface according to Eq. 3.2.

$$\Delta G^* = \frac{(F\omega^2\gamma_{net}^3)}{k_B T\sigma^2} \qquad \text{Eq 3.2}$$

Here *F* is a geometric parameter, ω is the molar volume, and σ is supersaturation. γ_{net} represents a summation of the interfacial energies between the solution (L), surface (S), and crystal (C) defined in Eq. 3.3, where *h* also represents a geometric parameter.

$$\gamma_{net} = \gamma_{LC} + h(\gamma_{SC} - \gamma_{SL}) \qquad \text{Eq. 3.3}$$

The addition of groups better suited for biomineralization, such as carboxylic acids, create more favorable surface interactions and increase the probability of nucleation[4]. This work grew calcite on the surface of click functionalized surfaces due to the previous

work our group has done with this crystal system and its prevalence in the field of biomineralization[5].

Calcite growth was performed using a diffusion-based method. Firstly, a 100 mL solution of 200 μM calcium chloride was prepared by diluting a 200 mM calcium chloride stock solution using 18 MΩ water. Strips of PDMS were functionalized using the click chemistry scheme discussed earlier and placed on a glass plate 0.5 cm apart. The glass plate was then inverted and suspended in a glass dish and placed into a sealable box of dimensions 20x27x14.5 cm. In the same box, two dishes were placed 7.5 cm apart and 16.5 cm from the dish containing the calcium chloride solution. In these two dishes was equal parts of 2 g of crushed ammonium carbonate. The box was then sealed, and the crystallization proceeded for 3 hours. After crystallization was performed samples were removed from the solution, placed onto clean microscope slides, and dried using N_2 gas.

Imaging was performed using a Zeiss Axio Scope A1 using an optical imaging procedure. Surfaces were observed using a 5x objective and brightfield parameters. Images taken with the microscope were then further processed using ImageJ to acquire information on the crystal count and size distribution in the area observed.

3.1.1 Results & Discussion

To achieve an understanding of how closely the click functionalized surfaces mimic previous work two functionalized surfaces (alcohol and carboxylic acid) and native PDMS were observed. When crystals were grown on the surface of PDMS functionalized with propargyl alcohol there was little crystal growth on the surface and those that did grow were relatively small (Figure 3.1 A). Considering, the surface

environment is decorated primarily with -OH groups and using contact angle it was evident the surface was mimicking oxidized PDMS this is to be expected. Oxidized PDMS is known to inhibit the growth of calcite on its surface due to its high surface energy from the -OH groups.

Surfaces decorated with carboxylic acid experienced far larger amounts of crystal growth and achieved an even smaller crystal size distribution than crystals grown on alcohol functionalized surfaces (Figure 3.1 B). Previous work studying calcium carbonate growth on carboxylic acid terminated surfaces showed a similar high degree of nucleation[6]. The degree of crystallinity was shown to be incredibly high and is not as well observed here. This could be attributed to a lack of appreciable time to allow the calcium carbonate to grow or the lack of rigidity on the surface may decrease the degree of crystallinity on the surface. Native PDMS served as a control since it is established that the native surface of PDMS encourages the growth of PDMS, which was replicated here (Figure 2.4 C).

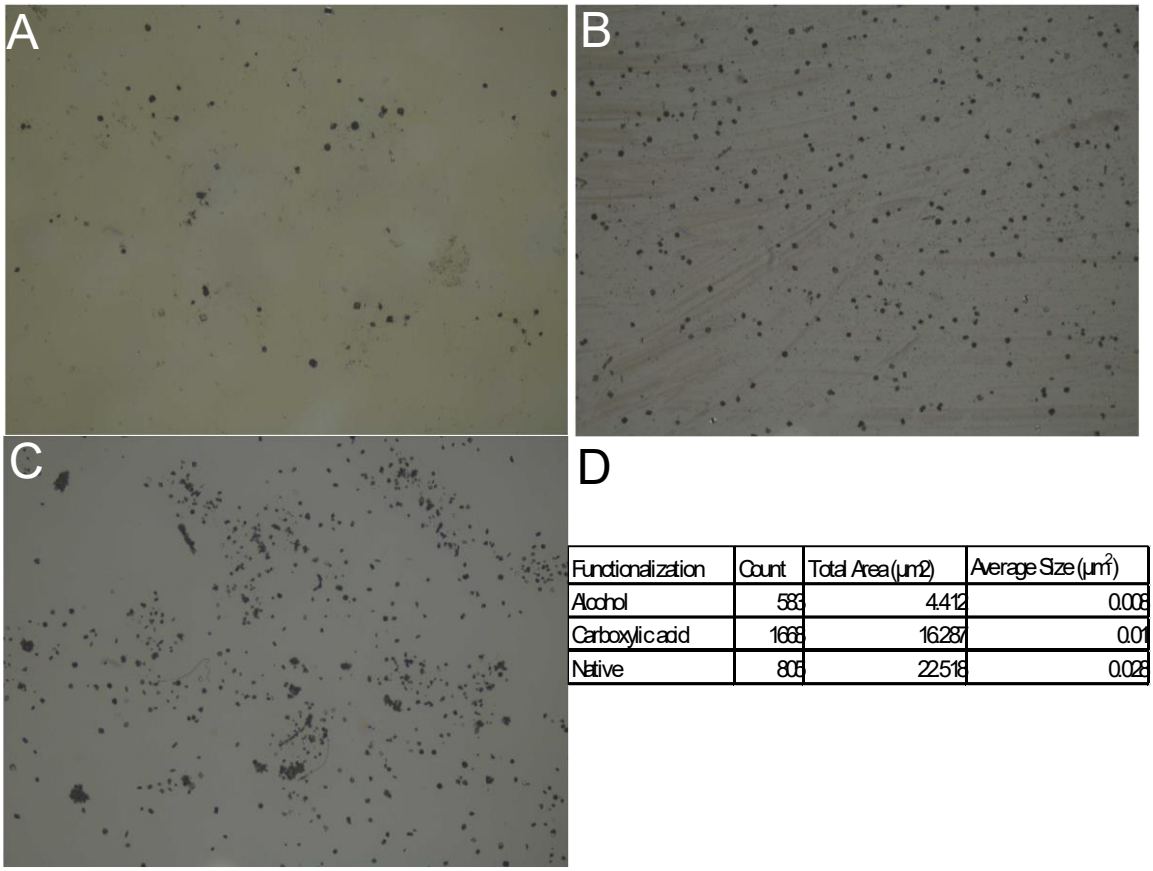

Functionalization	Count	Total Area (μm2)	Average Size (μm²)
Alcohol	583	4.412	0.008
Carboxylic acid	1668	16.287	0.01
Native	805	22.518	0.028

Figure 3.1 $CaCO_3$ growth on click functionalized PDMS A) 5x optical micrograph of $CaCO_3$ crystals grown on OH terminated PDMS. B) 5x optical micrograph of $CaCO_3$ crystals grown on COOH terminated PDMS. C) 5x optical micrograph of $CaCO_3$ crystals grown on CH_3 terminated PDMS. D) Table of results of crystal growth including count, area covered by crystals, and average crystal size distribution.

3.2 Kirigami and Chemical Patterning Adhesion

Kirigami allows for physical limitations to be placed on the area of adhesion experienced between to objects. By also exerting control over the chemical aspects of adhesion this can be tuned further. To achieve this, three patterns were printed onto the surface of PET to monitor how changing the areas of chemical adhesion effect the bonding between the surfaces (Figure 3.2 A-C). The areas in black are where ink was printed on the sample and the inscriber rectangular regions were removed with the craft cutter. Each design was also made to test for directional control of the release axis by changing the pattern orientation partway through the sample.

The adhesion between the PET sheets and the PDMS slab was measured using a Instron tensile strength tester. Samples were affixed to a stage using Kapton double sided tape due to its high adhesive force experienced with PDMS so that delamination between PDMS and PET, not PDMS and the stage, was being tested (Figure 3.2 D). Standard peel testing utilizes a moving stage to ensure a consistent peel angle of 90°, the Instron was used for ease of access but does not possess a moving stage leading to a variable peel angle and some artifacts in the results. Testing used a generic strain to break recipe where the stop point was when either complete delamination of the PET sheet or cohesive failure of the PDMS substrate occurred.

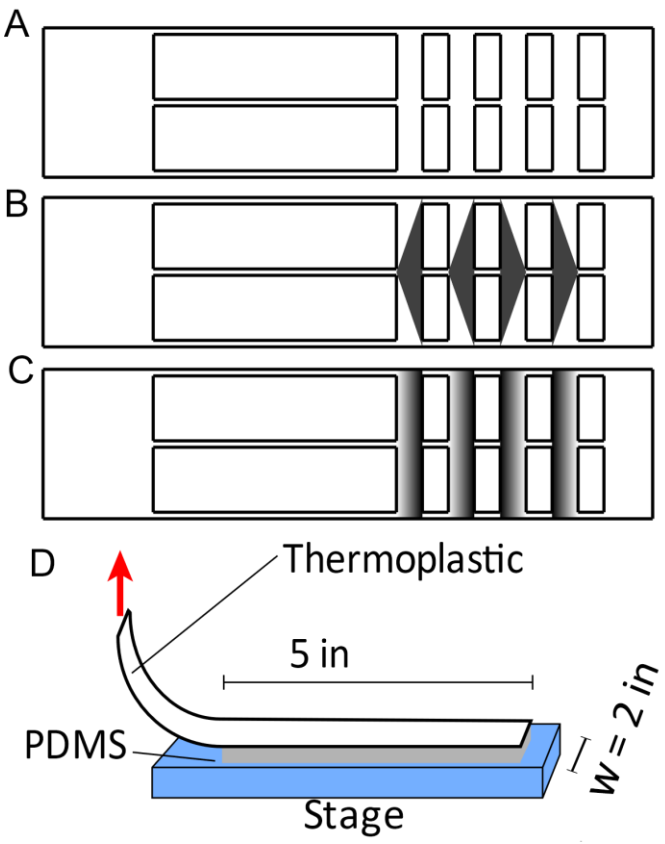

Figure 3.2 Illustration of pattern design and tensile testing design A-C) Designs printed onto PET sheets; either bare (A), triangle (B), or gradient (C). D) Orientation of composites on a tensile testing instrument. The arrow represents the direction of delamination.

3.2.1 Results & Discussion

As the PET sheets were delaminated from the surface 5 distinct force peaks were observed corresponding to the four areas with printed pattern and a fifth area that was an artifact of the design. Gradient patterned samples had an initial orientation where the first and second segments featured areas with little ink and therefore large initial adhesion. The third and fourth segments flip the design so instead of a large area of high adhesion a large segment of ink is encountered instead. The change in location of the area of strong adhesion cause a similar change in the peak force intensity experienced (Figure 3.3A). This was reflected in the delamination force profiles where the first two peaks feature a large initial area of adhesion which tapers off. The third and fourth peaks feature a lower initial force and lower force overall as the peel did not have to overcome a large adhesion barrier.

This result was shown to be even more drastic for the samples patterned with triangles. Here the area of area of programmed adhesion was initially larger than that experienced by the gradient pattern which was reflected in the large initial force reading recorded for this pattern (Figure 3.3B). As the pattern flipped, instead of needing to overcome an initial large adhesion area, a large area of no adhesion is experienced first and a lower force in general is required to finish delaminating the sample. All samples experience the same large delamination force for the final peak due to the end of all the samples bearing a large portion of complete adhesion requiring a maximum force to successfully finish the delamination.

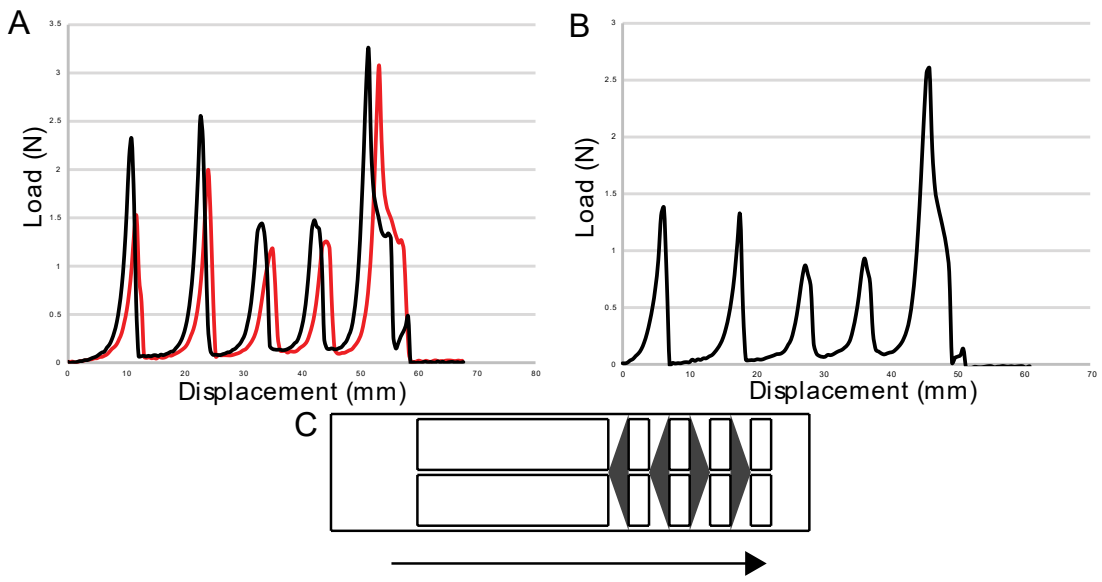

Figure 3.3 Delamination of patterned PET sheets from PDMS A) Force profile of triangle patterned samples. B) Force profile of a gradient patterned sample. C) Illustration of Triangle patterned sample with an arrow demonstrating direction of delamination.

References

1. Smeets, P. J. M.; Cho, K. R.; Kempen, R. G. E.; Sommerdijk, N. A. J. M.; De Yoreo, J. J.; Calcium Carbonate Nucleation Driven by Ion Binding in a Biomimetic Matrix Revealed by *In situ* Electron Microscopy. *Nature Materials*, **2015**, *14*, 394-399. DOI: 10.1038/NMAT4193
2. Giuffre, A. J.; Hamm, L. M.; Han, N.; De Yoreo, J. J.; Dove, P. M.; Polysaccharide Chemistry Regulates Kinetics of Calcite Nucleation Through Competition of Interfacial Energies. *PNAS*, **2013**, *110* (23), 9261-9266. DOI: 10.1073/pnas.1222162110
3. Teng, H. H.; Dove, P. M.; De Yoreo, J. J.; Kinetics of Calcite Growth: Surface Processes and Relationships to Macroscopic Rate Laws. *Geochimica et Cosmochimica Acta*, **2000**, *64* (13), 2255-2266. DOI: 10.1016/S0016-7037(00)00341-0
4. Travaille, A. M.; Kaptijn L.; Verwer, P.; Hulsken, B.; Elemans, J. A. A. W.; Nolte, R. J. M.; van Kempen H.; Highly Oriented Self-Assembled Monolayers as Templates for Epitaxial Calcite Growth. *J. Am. Chem. Soc.*, **2003**, *125* (38), 11571–11577. DOI: 10.1021/ja034624r
5. Taylor, J.M.; Konda, A.; Morin, S.A.; Spatiotemporal Control of Calcium Carbonate Nucleation Using Programmable Deformations of Elastic Surfaces. *Soft Matter* **2020**, *16*, 6038-6043. DOI: 10.1039/d0sm00734j
6. Aizenberg, J.; Black, A. J.; Whitesides, G. M.; Oriented Growth of Calcite Controlled by Self-Assembled Monolayers of Functionalized Alkanethiols Supported on Gold and Silver. *J. Am. Chem. Soc.* **1999**, *121* (18), 4500–4509. DOI: 10.1021/ja984254k

CHAPTER 4: FUTURE PROSPECTS OF PATTERNED CHEMICAL FUNCTIONALITY AND AHDESION

In previous chapters, schemes to modulate surface chemistry using click chemistry and methods of patterning chemical functionalization were discussed. These methods were then utilized for biomineralization and patterning adhesion towards the creation of composite materials that experience a quick release axis. The information gathered from these projects will be used in the future for work described in the following chapter.

4.1 Covalent Attachment of Hydrogels

Hydrogels are a classification of polymer that due to the porosity of the polymer network and the intrinsic hydrophilicity of the backbone can take up water causing the network to swell[1]. The swelling experienced is dependent on several factors such as crosslink density[2,3], monomer size, and for certain hydrogels temperature[4]. Poly (acrylamide), or PAm, is a hydrogel whose properties are well established in the literature, particularly its swelling and deswelling nature[5]. PAm hydrogels due to their structure swell in the presence of water due to the abundance of hydrogen bonding and ability of the polymer chain to flex and extend. When the hydrogel is subjected to an anhydrous solvent, such as ethanol, the removal of water from the hydrogel pores causes the matrix to shrink to its original state. A similar set of swelling characteristics is observed for poly (N-isopropyl acrylamide), or NIPAm[6]. While structurally similar to PAm, NIPAm does not contain proper functional groups to participate in hydrogen bonding. Instead, it experiences a phase change at approximately 32° C[7].

Despite the differences in the mechanism of swelling both hydrogels have been used for the creation of soft actuators[9-11]. Using the mimic masking techniques described earlier large patterns of wettability can be generated rapidly. Where previously this was used for the creation of large, ordered arrays of liquid droplets, if the droplets are, instead of water, a hydrogel pre-polymer mixture, a large array of hydrogels can be made just as easily[12]. With this large array of hydrogels now on the surface of oxidized PDMS they remain adhered mostly through non-covalent forces (Van der Waals and hydrogen bonding). The adhesive force they experience is still strong enough that when the phase transition mentioned previously is experienced, in this case by varying relative humidity, it causes a force imbalance with the surface of PDMS leading to buckling on the surface. This buckling was also shown to be directional by adjusting the size and directionality of the hydrogel droplets or adjusting the orientation of the mask prior to oxidation. Despite the advances this proposed in the field of soft robotics these actuators were unusable in aqueous environments due to the lack of covalent bonds between the hydrogel and PDMS. Integrating functional groups onto the surface of PDMS that allow for the formation of covalent bonds with the hydrogel network should allow for the creation of thin, soft actuators that function properly in aqueous environments.

4.1.1 Methods

Mimic masking allows for the selective oxidation and functionalization of PDMS. After oxidation, PDMS samples were functionalized using a liquid deposition procedure for silanization. This procedure included suspending oxidized samples of PDMS in 10 mL of a solution of 95:5 ethanol:water (v/v) and adding 200 μL of 3-(trimethoxylsilyl)

propyl methacrylate for 5 minutes. Following the deposition, the PDMS is removed from the solution, sprayed with ethanol, and placed in a 90°C oven for 5 minutes.

The two hydrogels used, PAm and NIPAm, were prepared by dissolving the monomer in water along with the photoinitiator, Irgacure 2959, and a crosslinker, bis-acrylamide. This pre-polymer mixture was the deposited onto functionalized PDMS using a nebulizer (Figure 4.1A). Following complete filling of the hydrogel spot, crosslinking was performed using a 1000W UV source.

4.1.2 Preliminary Results

Once the hydrogels were deposited and crosslinked to the surface, a simple wash step with deionized water was performed to test the hydrogels adhesion to the surface. The washing step involved submersion in de-ioninzed water followed by drying with a N_2 gas. Both the PAm and NIPAm hydrogels remained adhered to the surface of PDMS after the washing step. The array of the hydrogels was also well maintained after the washing step, ~99% remained attached. The hydrogels also remain adhered when subjected to a constant flow of water and not just simple submersion. The ability to remain adhered in a constant flow environment also allowed for demonstrations of their swelling and deswelling nature. PAm hydrogels could be swollen upon submersion in water and then shrunk by flowing over an organic solvent, ethanol, to remove water from the hydrogel and collapse the matrix.

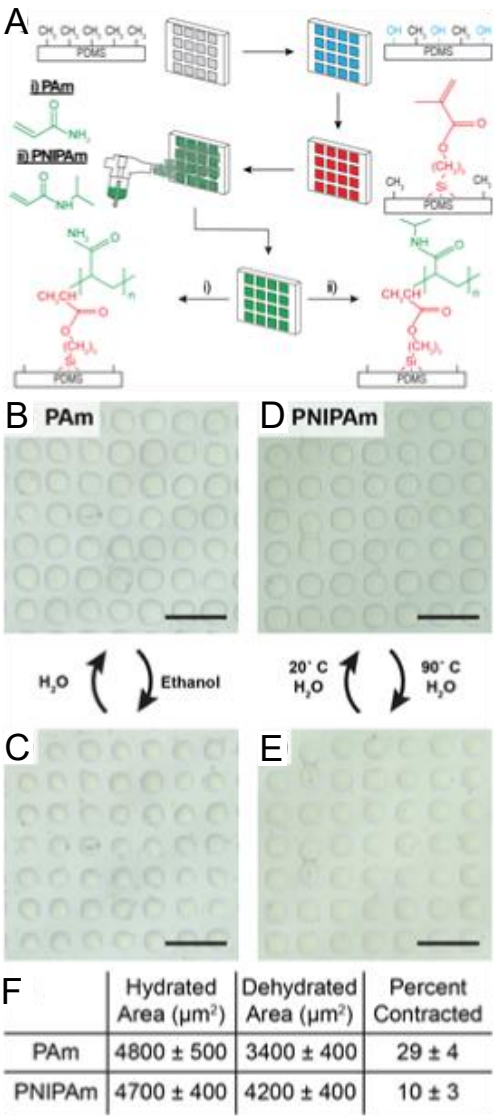

F	Hydrated Area (μm²)	Dehydrated Area (μm²)	Percent Contracted
PAm	4800 ± 500	3400 ± 400	29 ± 4
PNIPAm	4700 ± 400	4200 ± 400	10 ± 3

Figure 4.1 Covalent attachment of hydrogels that swell and deswell A) Illustration of the process to covalently attach both PAm (i) and NIPAm (ii). B-C) PAm hydrogels swollen under aqueous conditions (B) and shrunken in organic solvent (C). D-E) NIPAm hydrogels swollen under aqueous conditions (D) and shrunken in organic solvent (E). F) table quantifying the area change experienced by both PAm and NIPAm hydrogels.

The main advantage that these covalently bound hydrogels present is their ability to function while submerged in water. Their classical means of actuation however, typically involved the manipulation of temperature or relative humidity. Humidity is impossible to vary underwater so other means of actuation need to be used. Incorporating functional filler into the pre-polymer mix, like carbon nanotubes or platinum nanoparticles, can generate heat for actuation by other schemes, such as converting light into heat or highly exothermic chemical reactions occurring inside the hydrogel matrix. The catalytic decomposition of hydrogen peroxide (equation 4.1):

$$2H_2O_2(aq) \rightarrow 2H_2O(l) + O_2(g) \qquad \text{(Eq 4.1)}$$

is a highly exothermic catalytic process and an excellent test case.

To test the effectiveness of this process as a chemical engine, the original assembly needed to be tested first. When hydrogels are crosslinked to the surface of PDMS without platinum nanoparticle fillers and H_2O_2 is flowed over there is little change to the hydrogels. The area change of hydrogels with platinum was only 5%, less than previously recorded when water of varying temperatures was used (Figure 4.2 A, B, E). Meanwhile, when hydrogels were assembled with platinum nanoparticles two key differences were observed. First, the hydrogels experienced a percent area reduction closer, now 12%, to that observed when the temperature of water was changed. Second, the hydrogels now also evolved bubbles (Figure 4.2 C-E). One of the products of catalytic decomposition of hydrogen peroxide is O_2 gas. Therefore, the presence of gas bubbles is a positive indicator of successful decomposition.

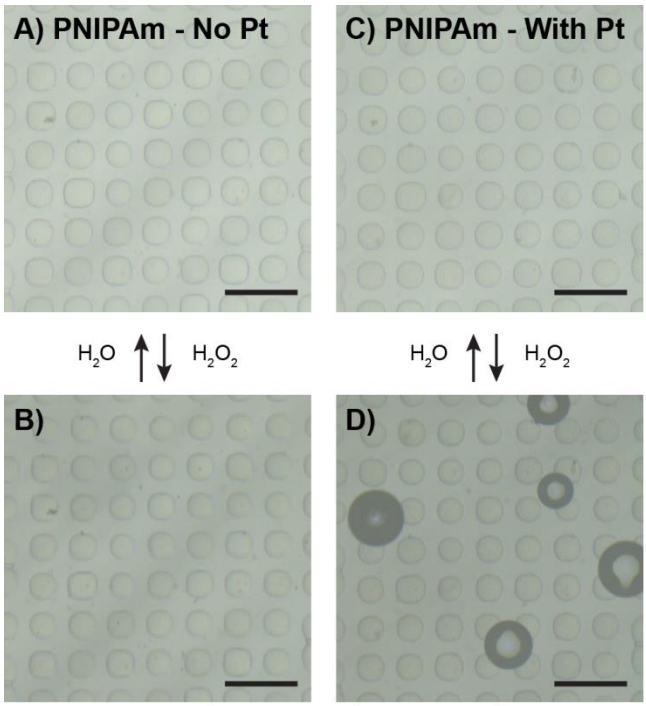

E)	Area in H_2O (μm²)	Area in H_2O_2 (μm²)	Percent Contraction
PNIPAm - No Pt	4600 ± 400	4400 ± 400	5 ± 3
PNIPAm - With Pt	4500 ± 400	4000 ± 400	12 ± 3

Figure 4.2 Chemically driven phase transition of covalently bound hydrogels A-B) NIPAm hydrogels covalently attached to functionalized PDMS without platinum nanoparticles in water (A) and 3% H_2O_2 (B). C-D) NIPAm hydrogels covalently attached to functionalized PDMS with platinum nanoparticles in water (C) and 3% H_2O_2 (D). E) Table calculating the percent area change of hydrogels in water vs. peroxide solution.

4.1.3 Future Work

Despite the positive results of these experiments, the decomposition of hydrogen peroxide is a poor reaction for thermal actuation. The evolution of gas, while a positive indicator of the reactions success, could disrupt the incorporation of these hydrogel systems in various applications. Moving to different chemical engines, that do form gaseous products, will allow for easier application of covalently bound hydrogels. This can be accomplished by using other highly exothermic reactions such as click reactions or looking at other means of heat generation, such as light conversion. These hydrogels also do not illicit as large an area change as PAm, leading to less of a response ratio when used for applications such as soft actuators. Applying this method to a more flexible hydrogel or taking inspiration from block copolymers and incorporating a more flexible monomer could allow for a greater response ratio.

4.2 Generation of Large Arrays of Hydrogels for 3D Cell Growth

Hydrogels also experience high biocompatibility due to their organic components and stability in water. Combining this with their intrinsic elasticity has led to their use in biomaterial applications. This has been done with creating smart bandages[14,15], soft biological implants[16,17], and semi-permeable membranes[18,19]. This exposes cells to materials that can experience variable stiffness[19,20], porosity[21,22], and swelling parameters[23]. While work has been done to investigate how cells behave while encapsulated in hydrogel systems, this is limited to bulk hydrogels[24]. Working with bulk hydrogels limits study of how changes to the surrounding environment effect cells on an induvial basis. Utilizing techniques developed for the covalent attachment of large arrays of hydrogels it should be easier to monitor cell reactions to environmental stimuli and

increase the throughput that these studies can be performed at due to number of spots each array features.

4.2.1 Methods

Functionalization of PDMS was carried out in the exact same manner as covalent attachment of hydrogels. PDMS strips were selectively oxidized using a mimic mask and then submerged in 10 mL of 95:5 (v/v) water and ethanol solution with 200 μL of 3-(trimethoxylsilyl) propyl methacrylate for 5 minutes. After deposition samples were rinsed with ethanol and transferred to a 90°C oven for 5 minutes to finish the functionalization.

The pre-polymer mix was prepared by dissolving 100 mg of Irgacure 2959 in 1 mL of methanol. In a separate container the PEGDA solution was prepared by dissolving enough PEGDA to achieve the appropriate concentration (between 3-50% w/w) in 1 mL of phosphate buffer solution (pH 7). After addition of PEGDA at higher concentrations the solution needed vigorous stirring to achieve complete dissolution. Once the PEGDA was dissolved completely, 10 μL of the Irgacure solution were added to achieve a final concentration of 1% Irgacure (w/w). The final solution was syringe filtered and then transferred to a 1 mL syringe for spray application.

The hydrogel pre-polymer mix was spray deposited on the surface using a nebulizer according to procedures previously developed by our group. Samples were sprayed with the hydrogel pre-polymer mixture for 2.5 minutes and then observed for underfilling or overfilling of the pattern. If the pattern spots were underfilled the sample was sprayed again in intervals of 30 seconds until filled completely. When satisfactorily

filled the samples were removed from the spray deposition chamber and crosslinked using a 200 W 365 nm UV source oriented beneath the sample to facilitate reactivity with the surface first. Crosslinking was performed for 4 minutes to allow for maximum exposure time without harming cells.

4.2.2 Results & Discussion

Initially, the dry adhesion of hydrogels was tested using the tape test. The tape was performed by first imaging hydrogels under a laser confocal microscope, applying and removing a piece of 3M scotch tape, and then reimaging the initial observed area. The first set of parameters tested was how necessary the various steps of the functionalization procedure were for the attachment of hydrogels to the surface. This entailed studying surfaces that had not been treated with the silane and hydrogels where the crosslinking was not performed. Hydrogels spray deposited onto oxidized surfaces and then crosslinked, experienced some adhesion to the surface but a significant portion of the array was still lost (Figure 4.3 A-B). When hydrogels were not crosslinked the polymer, network did not have a chance to properly form and remained in a liquid state (Figure 4.3 C-D). Only samples where the adhesion promoting silane was deposited onto the surface saw complete retention of the hydrogel array and experienced little to no deformation of the hydrogel structure after removal of the tape (Figure 4.3 E-F).

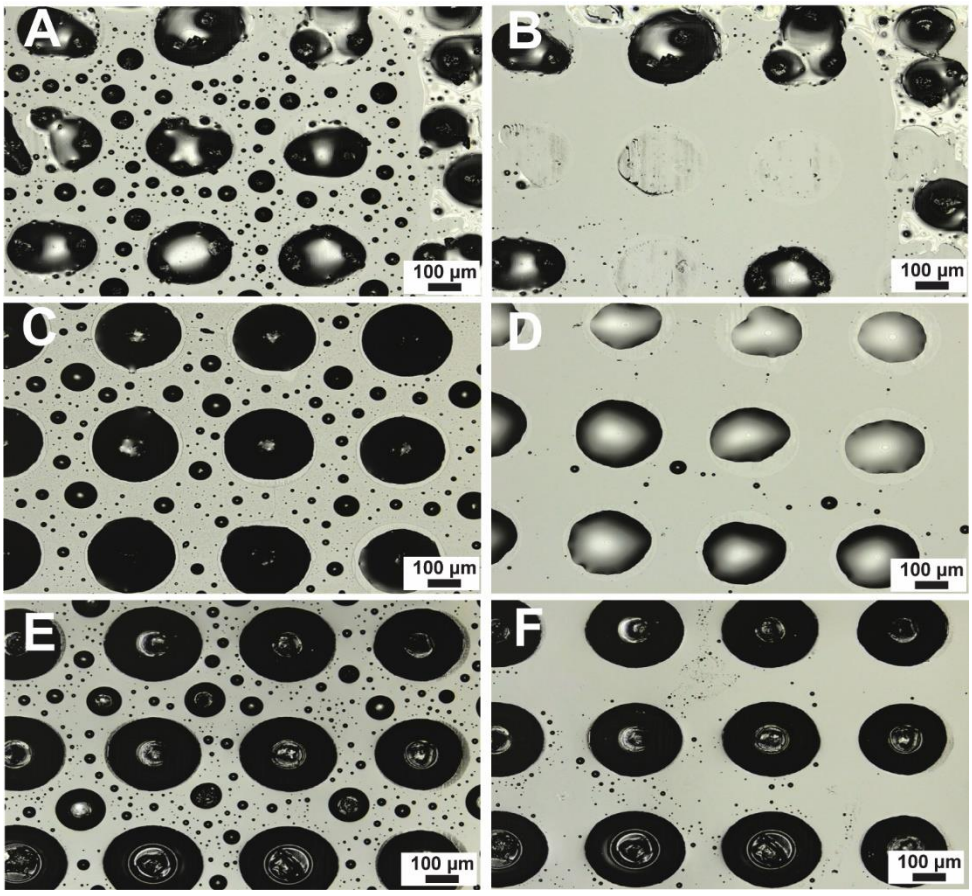

Figure 4.3 Functionalization effect on hydrogel adhesion A-B) Adhesion PEGDA hydrogels to the surface of oxidized PDMS before (A) and after (B) application and removal of tape. C-D) Adhesion of uncrosslinked PEGDA hydrogels to methacrylate terminated PDMS before (C) and after (D) application and removal of tape. E-F) Adhesion of PEGDA hydrogels to methacrylate terminated PDMS before (E) and after (F) application and removal of tape. Scale represent 100 µm.

To gain understanding of how the polymer network forms with the surface the concentrations of both PEGDA and Irgacure. When the concentration of Irgacure is too low, 0.05-0.15% (w/w), the hydrogel is notable to properly crosslink. This causes the hydrogel droplets to remain liquid and not bind to the surface (Figure 4.4 A-D). Adhesion of hydrogels to the surface was accomplished with a higher concentration of Irgacure, 1% (w/w) (Figure 4.4 E-F). A similar condition is seen with respect to monomer concentration and adherence to the surface. When the concentration of PEGDA was kept below 10% (w/w) hydrogels experienced adhesion to the surface as expected (Figure 4.4 A-D). When the concentration was raised to 30% (w/w) once again the droplets did not properly crosslink and remained in a liquid state (Figure 4.4 E-F). Interestingly, when the concentration of PEGDA was raised even further, 50% (w/w), the viscosity of the hydrogel solution was so great that the droplets were able to bridge the unfunctionalized gap (Figure 4.4 G). This led to the formation of far larger droplets that were able to be internally crosslinked and crosslinked to the surface (Figure 4.4 H).

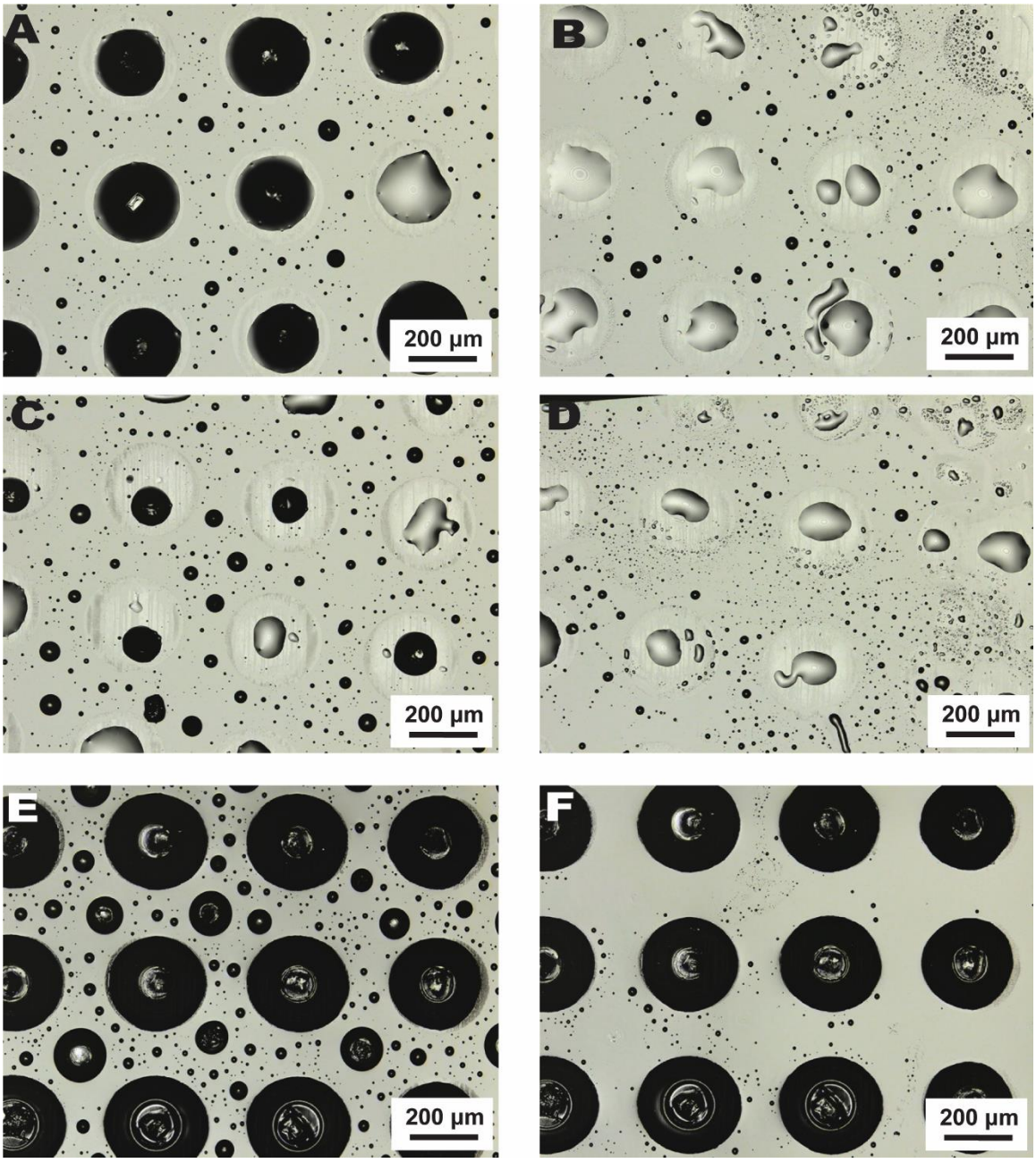

Figure 4.3 Photoinitiator concentration effecting dry adhesion of hydrogels A-B) Hydrogels containing 0.05% Irgacure before (A) and after (B) application and removal of tape. C-D) Hydrogels containing .015% Irgacure before (C) and after (D) application and removal of tape. E-F) Hydrogels containing 1% Irgacure before (E) and after (F) application and removal of tape.

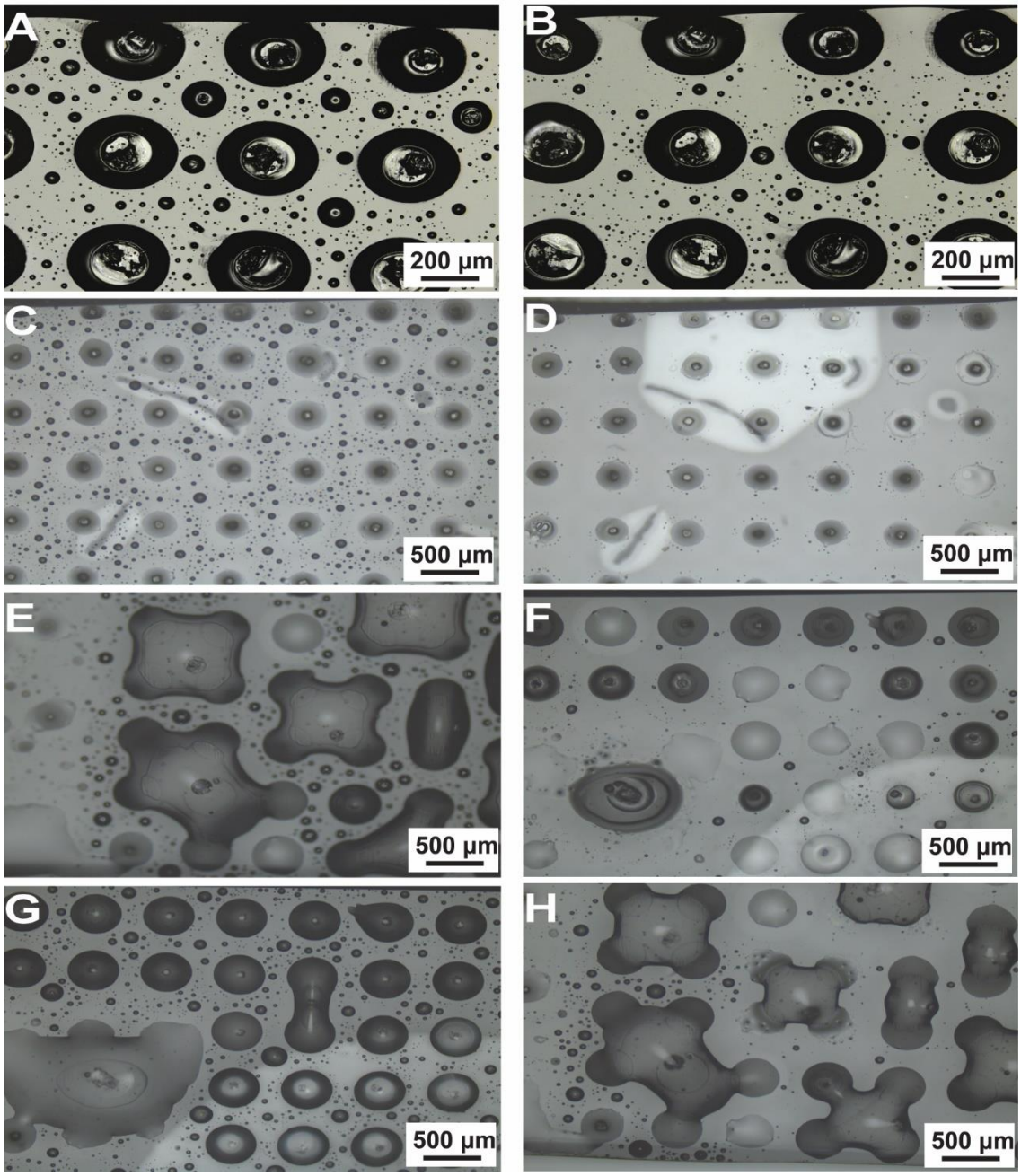

Figure 4.4 Monomer concentration effecting dry adhesion of hydrogels A-B) Hydrogels containing 3% PEGDA before (A) and after (B) application and removal of scotch tape. C-D) Hydrogels containing 10% PEGDA before (C) and after (D) application and removal of scotch tape. E-F) Hydrogels containing 30% PEGDA before (E) and after (F) application and removal of scotch tape. G-H) Hydrogels containing 50% PEGDA before (G) and after (H) application and removal of scotch tape.

Wet adhesion of the hydrogels was also a concern since cells need to be submerged in proper growth media to proliferate and grow. This required that along with dry adhesion, the wet adhesion of hydrogels also needed to be monitored. Wet adhesion followed a similar pattern to dry adhesion, where if the hydrogel did not appear to feature a morphological change, the hydrogel remained adhered after submersion for 48 hours in water (Figure 4.5 A-B). The largest difference was that instead of a morphological change, the hydrogel droplets were completely washed away from the surface. If a hydrogel was able to remain adhered after the tape test it was found to also remain adhered after submersion in water.

With the aim of these hydrogels to eventually involve the incorporation of cells, who do not grow in water, the stability of hydrogels in other solvents needed to be performed. Cells are often grown in a cell growth media, such as Dulbecco's modified eagle medium (DMEM), which contain a complex mixture of various salts and proteins for the cells. This added complexity was shown to not affect the adhesion of PEGDA hydrogels over a 48-hour period at elevated temperatures, 38° C (Figure 4.5 C-D). To help ensure the safe growth of the cells an antibiotic, penicillin-streptomycin (penstrip), and fetal bovine serum (FBS) were also added to the growth solution and still did not interfere with the adhesion of PEGDA hydrogels (Figure 4.5 E-F).

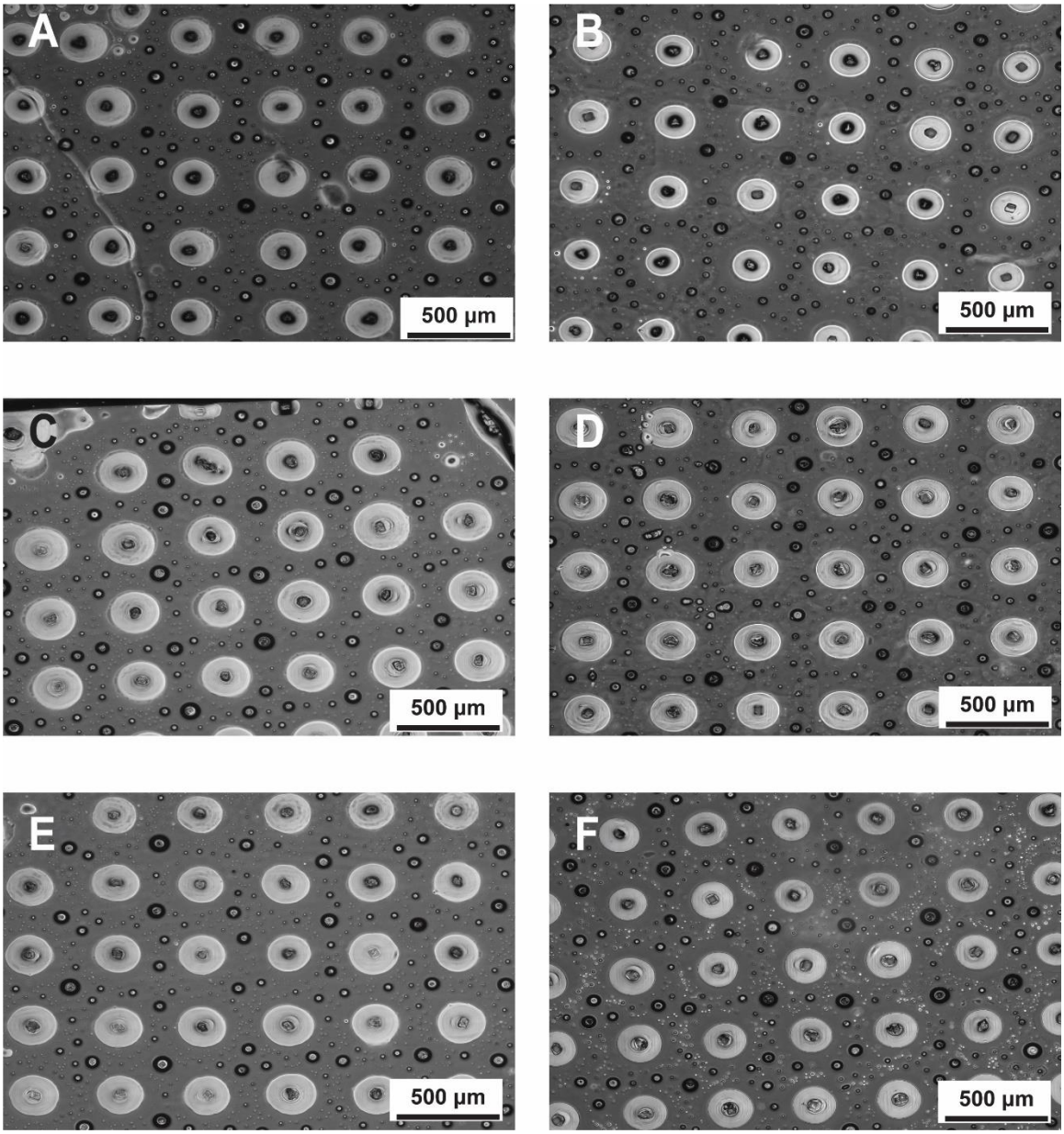

Figure 4.5 Wet adhesion of PEGDA hydrogels in various media A-B) PEGDA hydrogels submerged in water before (A) and after (B) 48 hours at 38°C. C-D) PEGDA hydrogels submerged in DMEM before (C) and after (D) 48 hours at 38°C. PEGDA hydrogels submerged in DMEM with penstrip and FBS before (A) and after (B) 48 hours at 38°C.

There has been significant work done to covalently bind a biocompatible hydrogel, PEGDA, to the surface of PDMS. Despite this, incorporation of cells into the hydrogels is a difficult task as they can affect the rheological properties necessary for spray deposition. PEGDA itself also does not encourage the attachment of proliferation of cells making. PEGDA can be further modified with RGD, a cell adhesion promoter, allowing for cell proliferation inside the hydrogel matrix. There is also further tuning of the hydrogel network to understand how cells proliferate while confined in small spaces with variable stiffness or porosity.

References

1. Ruel-Gariépy, E.; Leroux, J.-C.; In situ-Forming Hydrogels—Review of Temperature-Sensitive Systems. *European Journal of Pharmaceutics and Biopharmacuetics*, **2004**, *58* (2), 409-426. DOI: 10.1016/j.ejpb.2004.03.019
2. Xue, W.; Champ, S.; Huglin, M. B.; Network and Swelling Parameters of Chemically Crosslinked Thermoreversible Hydrogels. *Polymer*, **2001**, *42* (8), 3665-3669. DOI: 10.1016/S0032-3861(00)00627-3
3. Atta, A. M.; Abdel-Azim, A.-A. A.; Effect of Crosslinker Functionality on Swelling and Network Parameters of Copolymeric Hydrogels. *Polymers for Advanced Technologies*, **1998**, *9* (6), 340-348. DOI: 10.1002/(SICI)1099-1581(199806)9:6<340::AID-PAT787>3.0.CO;2-F
4. Emileh, A.; Vasheghani-Farahani, E.; Imani, M.; Swelling Behavior, Mechanical Properties and Network Parameters of pH- and Temperature-Sensitive Hydrogels of Poly ((2-dimethyl amino) ethyl methacrylate-*co*-butyl methacrylate). *European Polymer Journal*, **2007**, *43* (5), 1986-1995. DOI: 10.1016/j.eurpolymj.2007.02.002
5. Peters, A.; Candau, S. J.; Kinetics of Swelling of Polyacrylamide Gels. *Macromolecules* **1986**,*19*, 1952-1955. DOI: 10.1021/ma00161a029
6. Crowther, H. M.; Vincent, B.; Swelling Behavior of Poly- *N*-isopropylacrylamide Microgel Particles in Alcoholic Solutions. *Colloid and Polymer Science*, **1998**, *276*, 46-51. DOI: 10.1007/s003960050207
7. Kokufuta, E.; Zhang, Y.-Q.; Tanaka, T.; Mamada, A.; Effects of Surfactants on the Phase Transition of Poly(N-isopropylacrylamide) Gel. *Macromolecules*, **1993**, *26*, 1053-1059.
8. Guo, M.; Wu, Y.; Xue, S.; Xia, Y.; Yang, X.; Dzenis, Y.; Li, Z.; Lei, W.; Smith, A. T.; Sun, L.; A highly Stretchable, Ultra-Tough, Remarkably Tolerant, and Robust Self-Healing Glycerol-Hydrogel for a Dual-Responsive Soft Actuator. *J. Mater. Chem. A*, **2019**, ***7***, 25969-25977. DOI: 10.1039/C9TA10183G
9. Kim, J.; Kim, J.-W.; Kim, H. C.; Ko, H.-U; Muthoka, R. M.; Review of Soft Actuator Materials. *International Jounral of Precision Engineering and Manufacturing*, **2019**, *20*, 2221-2241.DOI: 10.1007/s12541-019-00255-1
10. Zhang, E.; Wang, T.; Hong, W.; Sun, W.; Liu, X.; Tong, Z.; Infrared-Driving Actuation Based on Bilayer Graphene Oxide-poly(N-isopropylacrylamide) Nanocomposite Hydrogels. *J. Mater. Chem. A*, **2014**, *2*, 15633-15639. DOI: 10.1039/C4TA02866J
11. Peng, X.; Jiao, C.; Zhao, Y.; Chen, N.; Wu, Y.; Liu, T.; Wang H.; Thermoresponsive Deformable Actuators Prepared by Local Electrochemical Reduction of Poly(*N*-isopropylacrylamide)/Graphene Oxide Hydrogels. *ACS Appl. Nano Mater.* **2018**, *1* (4), 1522–1530. DOI: 10.1021/acsanm.8b00022
12. Bowen, J.J.; Rose, M.A.; Konda, A.; Morin, S.A.; Surface Molding of Microscale Hydrogels with Microactuation Functionality. *Angew. Chem. Int. Ed.*, **2018**, *57*,1236 –1240. DOI: 10.1002/anie.201710612

13. Plauck, A.; Stangland, E. E.; Dumesic, J. A.; Mavrikakis, M.; Active Sites and Mechanisms for H_2O_2 Decomposition Over Pd Catalysts. *PNAS*, **2016**, *113* (14), 1973-1982. DOI: 10.1073/pnas.1602172113
14. Mostafalu, P.; Tamayol, A.; Rahimi, R.; Ochoa, M.; Khalilpour A.; Kiaee, G.; Yazdi, I. K.; Bagherifard, S.; Dokmeci M. R.; Ziaie, B.; Sonkusale, S. R.; Khademhosseini, A.; Smart Bandage for Monitoring and Treatment of Chronic Wounds. *Small*, **2018**, *14* (33), 1703509. DOI: 10.1002/smll.201703509
15. Kassal, P.; Zubak, M.; Scheipl, G.; Mohr, G.J.; Steinberg, M. D.; Steinberg, I. M.; Smart Bandage with Wireless Connectivity for Optical Monitoring of pH. *Sensors and Actuators B: Chemical*, **2017**, *246*, 455-460. DOI: 10.1016/j.snb.2017.02.095
16. Peattie, R. A.; Rieke, E. R.; Hewett, E. M.; Fisher, R. J.; Chu, X. Z.; Prestwich, G. D.; Dual Growth Factor-Induced Angiogenesis In Vivo Using Hyaluronan Hydrogel Implants. *Biomaterials*, **2006**, *27* (9), 1868-1875. DOI: 10.1016/j.biomaterials.2005.09.035
17. Obiweluozor, F. O.; Tiwari, A. P.; Lee, J.; H.; Batgerel, T.; Kim, J. Y.; Lee, D.; Park, C. H.; Kim, C. S.; Thromboresistant Semi-IPN Hydrogel Coating: Towards Improvement of the Hemocompatibility/Biocompatibility of Metallic Stent Implants. *Materials Science and Engineering: C*, **2019**, *99*, 1274-1288. DOI: 10.1016/j.msec.2019.02.054
18. Schmitt, B.; Alexandre, E.; Boudjema,K.; Lutz, P. J.; Poly(ethylene oxide) Hydrogels as Semi-Permeable Membranes for an Artificial Pancreas. *Macromolecular Bioscience*, **2002**, *2* (7), 341-351. DOI: 10.1002/1616-5195(200209)2:7<341::AID-MABI341>3.0.CO;2-4
19. Nafea, E. H.; Poole-Warren, L. A.; Martens, P. J.; Immunoisolating Semi-Permeable Membranes for Cell Encapsulation: Focus on Hydrogels. *Journal of Controlled Release*, **2011**, *154* (2), 110-122. DOI: 10.1016/j.jconrel.2011.04.022
20. Accardo, J. V.; Kalow, J. A.; Reversibly Tuning Hydrogel Stiffness Through Photocontrolled Dynamic Covalent Crosslinks. *Chem. Sci.*, **2018**, *9*, 5987-5993. DOI: 10.1039/C8SC02093K
21. Jaspers, M.; Rowan, A. E.; Kouwer, P. H. J.; Tuning Hydrogel Mechanics Using the Hofmeister Effect. *Adv. Funct. Mater*. **2015**, *25*, 6503–6510. DOI: 10.1002/adfm.201502241
22. Dewavrin, J.-Y.; Hamzavi, N.; Shim, V. P. W.; Raghunath, M.; Tuning the Architecture of Three-Dimensional Collagen Hydrogels by Physiological Macromolecular Crowding. *Acta Biomaterialia*, **2014**, *10* (10), 4351-4359. DOI: 10.1016/j.actbio.2014.06.006
23. Hoshino, K.-i.; Nakajima, T.; Matsuda, T.; Sakai, T.; Gong, J. P.; Network Elasticity of a Model Hydrogel as a Function of Swelling Ratio: from Shrinking to Extreme Swelling States. *Soft Matter*, **2018**, *14*, 9693-9701. DOI: 10.1039/C8SM01854E
24. Lozoya, O. A.; Wauthier, E.; Turner, R. A.; Barbier, C.; Prestwich, G. D.; Guilak, F.; Superfine, R.; Lubkin, S. R.; Reid, L. M.; Regulation of Hepatic Stem/Progenitor Phenotype by Microenvironment Stiffness in Hydrogel

Models of the Human Liver Stem Cell Niche. *Biomaterials*, **2011**, *32* (30), 7389-7402. DOI: 10.1016/j.biomaterials.2011.06.042